FOSFODIESTERASAS DEL AMPc Y DEL GMPc EN EL CEREBRO: EXPRESIÓN EN PROCESOS NEUROINFLAMATORIOS Y NEURODEGENERATIVOS

Elisabet Reyes Irisarri
Barcelona 2007

Resultados

Trabajo 1:

Neuronal expression of cAMP-specífic phosphodiesterase 7B in the rat brain

Elisabet Reyes-Irisarri, Silvia Pérez-Torres, Guadalupe Mengod.

Publicado en *Neuroscience* 132 (2005) 1173-1185

Neuroscience 132 (2005) 1173–1185

NEURONAL EXPRESSION OF cAMP-SPECIFIC PHOSPHODIESTERASE 7B mRNA IN THE RAT BRAIN

E. REYES-IRISARRI, S. PÉREZ-TORRES AND G. MENGOD*

Department of Neurochemistry, Institut d'Investigacions, Biomèdiques de Barcelona, Consejo Superior de Investigaciones Científicas, Institut d'Investigacions Biomèdiques August Pi i Sunyer (IIBB-CSIC, IDIBAPS), c/Rosselló 161, 6°, E-08036 Barcelona, Spain

Abstract—cAMP plays an important role as second messenger molecule controlling multiple cellular processes in the brain. cAMP levels depend critically on the phosphodiesterases (PDE) activity, enzymes responsible for the clearance of intracellular cAMP. We have examined the regional distribution and cellular localization of mRNA coding for the cAMP-specific phosphodiesterase 7B (PDE7B) in rat brain by *in situ* hybridization histochemistry. PDE7B mRNA is specifically distributed in rat brain, preferentially in neuronal cell populations. The highest levels of hybridization are observed in olfactory tubercle, islands of Calleja, dentate gyrus, caudate-putamen and some thalamic nuclei. Positive hybridization signals are also detected in other areas, such as cerebral cortex, Purkinje cells of the cerebellum and area postrema. By double *in situ* hybridization histochemistry, we found that 74% and 79% of the cells expressing PDE7B mRNA in striatum and olfactory tubercle, respectively, were GABAergic cells (expressing glutamic acid decarboxylase mRNA), in contrast with the lack of expression in the few cholinergic cells (expressing choline acetyltransferase mRNA) present in those two areas (around 0.4% in olfactory tubercle). In the thalamic nuclei, a majority of cells containing PDE7B mRNA also expresses a glutamatergic marker (76.7% express vesicular glutamate transporter vGluT1 and 76% express vGluT2 mRNAs). Almost all PDE7B expressing cells in dentate gyrus (93%) were glutamatergic.

These results offer a neuroanatomical and neurochemical base that will support the search for specific functions for cAMP dependent PDEs and for the development of specific PDE7 inhibitors.

Key words: *in situ* hybridization, PDE, glutamatergic cells, GABAergic cells, cholinergic cells.

cAMP and cGMP play a key role in signal transduction in a wide variety of cellular responses. In brain, cAMP has been implicated in sensory functions, synaptic plasticity, learning and memory. Thus, information about how the intracellular cAMP levels are regulated will help to understand the mechanisms underlying these functions. Intracellular levels of cAMP are controlled not only by its synthesis by the enzyme adenylyl cyclase (Houslay and Milligan, 1997), but also by its degradation through the action of cyclic nucleotide phosphodiesterases (PDE), which catalyze the hydrolysis of 3′,5′-cyclic nucleotides into 5′-nucleoside monophosphates (Beavo, 1995; Conti and Jin, 1999; Francis et al., 2002; Houslay, 1998).

PDEs have been so far classified into 11 families (PDE1–PDE11). They have different regulatory properties and intracellular location, with particular isoforms being expressed in a cell-specific manner (Conti and Jin, 1999). Families 4, 7 and 8 specifically hydrolyze cAMP, with PDE7 and PDE8 having a higher affinity for this substrate. Two members of the PDE7 family have been cloned, PDE7A (Michaeli et al., 1993), and PDE7B (Hetman et al., 2000; Sasaki et al., 2000). The distribution of PDE7A transcripts in the CNS, was first determined in mouse brain by RNase protection assays (Bloom and Beavo, 1996). Later, PDE7A mRNA was visualized by *in situ* hybridization in a preliminary study in a few adult and embryonic rat brain regions (Hoffmann et al., 1998), in rat brain and peripheral organs (Miró et al., 2001), and in some areas of the human brain (Pérez-Torres et al., 2003). Recently, alterations on the mRNA levels of PDE7A in postmortem human brains with Alzheimer's disease has been reported (Pérez-Torres et al., 2003).

Different *in vivo* models have been developed suggesting an implication of cAMP in learning, memory processes and other brain functions. Treatment of aged mice with rolipram, a PDE4 inhibitor, ameliorated the physiological and the memory defects of the age-related spatial memory loss (Bach et al., 1999). Administration of rolipram, a selective PDE4 inhibitor, induced long-term potentiation in the CA1 field of mouse hippocampus (Barad et al., 1998). These findings suggest the involvement of cAMP in synaptic plasticity during learning and memory processes. Since PDE7 has high affinity for cAMP, this enzyme could play an important role in maintaining cAMP levels at the basal intracellular levels. It has been shown that PDE 7A plays a role in the activation and/or proliferation of T cells (Li et al., 1999) and is upregulated in human B-lymphocytes (Lee et al., 2002). A few PDE7 inhibitors have been described (Barnes et al., 2001; Castro et al., 2001; Martinez et al., 2000; Pitts et al., 2004).

The cellular localization of the PDEs in brain is an important step forward for the understanding of their function. Here we describe experiments aimed at the analysis of both regional and cellular expression of the mRNA coding for PDE7B in neuronal populations expressing specific neurotransmitters of the adult rat brain. Our study

*Corresponding author. Tel: +34-933-63-8323; fax: +34-933-63-8301.
E-mail address: gmlnqr@iibb.csic.es (G. Mengod).

Abbreviations: AC, adenylyl cyclase; ChAT, choline acetyltransferase GAD, glutamic acid decarboxylase; GFAP, glial fibrillary acidic protein; MBP, myelin binding protein; PBS, phosphate-buffered saline; PDE, phosphodiesterase; vGluT1, vesicular glutamate transporter 1; vGluT2, vesicular glutamate transporter 2.

0306-4522/05$30.00+0.00
doi:10.1016/j.neuroscience.2005.01.050

reveals that PDE7B mRNA has a restricted distribution in the brain being especially abundant in forebrain structures, where it is expressed in different neuronal populations with excitatory and inhibitory neurotransmitters.

EXPERIMENTAL PROCEDURES

Tissue preparation

Adult male Wistar rats ($n=5$; 200–300 g) were purchased from Iffa Credo (Lyon, France). Animal care followed the Spanish legislation on "Protection of animals used in experimental and other scientific purposes" in agreement with the European (E.E.C) regulations (O.J. of E.C. L358/1 18/12/1986). The animals were killed by decapitation. All efforts were made to minimize the number of animals used and their suffering. The brains were frozen on dry ice and kept at −20 °C. Tissue sections, 14 μm thick, were cut on a microtome-cryostat (Microm HM500 OM, Walldorf, Germany), thaw-mounted onto APTS (3-aminopropyltriethoxysilane; Sigma, St. Louis, MO, USA) -coated slides, and kept at −20 °C until used.

Hybridization probes

For the detection of PDE7B mRNA two 45 base-oligodeoxyribonucleotides that were complementary to bases 556–600 and 1390–1434 (GenBank acc. no. NM_080894) were used. These regions were chosen because they share no similarity with other members of the different PDE families. Most of the results shown in the present work were done using the first PDE7B oligonucleotide.

Glutamatergic cells were recognized by the presence of the mRNA coding for both vesicular glutamate transporters (vGluT1 and vGluT2): vGluT1 with two oligonucleotides complementary to bases 127–172 and 1756–1800 (GenBank acc. no U07609) and vGluT2 with two oligonucleotides complementary to the bases 466–510 and 2156–2200 (GenBank acc. no AF271235). GABAergic cells were identified by the presence of the enzyme synthesizing GABA, glutamic acid decarboxylase (GAD) that in adult brain exists as two major isoforms, GAD65 and GAD67. Two oligonucleotides for each isoform mRNA were made: bp 159–213 and 514–558 (GenBank acc. no NM_012563) and bp 191–235 and 1600–1653 (GenBank acc. no NM_017007). Cholinergic cells were distinguished by the presence of the enzyme choline acetyltransferase (ChAT) mRNA with two oligonucleotides complementary to bases 571–618 and 1321–1368 of the rat ChAT cDNA sequence (Ishii et al., 1990).

We also identified the non-neuronal population by the presence of the glial fibrillary acidic protein (GFAP) and myelin binding protein (MBP) mRNAs, markers for astrocytes and oligodendrocytes, respectively. Two oligonucleotides complementary to bases 225–274 and 1194–1242 were made for the GFAP mRNA (Brenner et al., 1990) and one oligonucleotide complementary to bases 179–223 (GenBank acc. no M25889) for MBP mRNA. The oligonucleotides were all synthesized and HPLC purified by Isogen Bioscience BV (Maarsden, The Netherlands). Evaluation of the oligonucleotide sequences with basic local alignment search tool of EMBL and GenBank databases indicated that the probes do not show any significant similarity with mRNAs other than their corresponding targets in the rat.

Oligonucleotides for PDE7B mRNA were labeled at their 3′-end using [α-^{33}P]dATP (3000 Ci/mmol; New England Nuclear, Boston, MA, USA) for the *in situ* hybridization histochemistry experiments and terminal deoxynucleotidyltransferase (Oncogene Research Products, San Diego, CA, USA), purified using QIAquick Nucleotide Removal Kit (Qiagen GmbH, Hilden, Germany; Tomiyama et al., 1997). ChAT, GAD and vGluT oligonucleotides (100 pmol) were non-radioactively labeled with the same enzyme and Dig-11-dUTP (Roche Diagnostics GmbH, Mannheim, Germany) according to a previously described procedure (Schmitz et al., 1991).

In situ hybridization histochemistry procedure

The protocols for single- and double-label *in situ* hybridization histochemistry were based on previously described procedures (Landry et al., 2000; Tomiyama et al., 1997) and have been already published (Serrats et al., 2003). Frozen tissue sections were brought to room temperature, fixed for 20 min at 4 °C in 4% paraformaldehyde in phosphate-buffered saline (PBS; 1× PBS: 8 mM Na_2HPO_4, 1.4 mM KH_2PO_4, 136 mM NaCl, 2.6 mM KCl), washed for 5 min in 3× PBS at room temperature, twice for 5 min each in 1× PBS, and incubated for 2 min at 21 °C in a solution of predigested pronase (Calbiochem, San Diego, CA, USA) at a final concentration of 24 U/ml in 50 mM Tris–HCl pH 7.5, 5 mM EDTA. The enzymatic activity was stopped by immersion for 30 s in 2 mg/ml glycine in 1× PBS. Tissues were finally rinsed in 1× PBS and dehydrated through a graded series of ethanol. For hybridization, radioactively labeled and non-radioactively labeled probes were diluted in a solution containing 50% formamide, 4× SSC (1× SSC: 150 mM NaCl, 15 mM sodium citrate), 1× Denhardt's solution (0.02% Ficoll, 0.02% polyvinylpyrrolidone, 0.02% bovine serum albumin), 10% dextran sulfate, 1% sarkosyl, 20 mM phosphate buffer pH 7.0, 250 μg/ml yeast tRNA and 500 μg/ml salmon sperm DNA. The final concentrations of radioactive and Dig-labeled probes in the hybridization buffer were in the same range (approximately 1.5 nM). Tissue sections were covered with hybridization solution containing the labeled probe/s, overlaid with Nescofilm coverslips (Bando Chemical Inc., Kobe, Japan) and incubated overnight at 42 °C in humid boxes. Sections were washed four times (15 min each) in 0.6 M NaCl, 10 mM Tris–HCl pH 7.5 at 60 °C, and once in the same buffer at room temperature for 30 min.

Development of radioactive and non-radioactive hybridization signal

Hybridized sections were treated as described by Landry et al., 2000. Briefly, after washing, the slides were immersed for 30 min in a buffer containing 0.1 M Tris–HCl pH 7.5, 1 M NaCl, 2 mM $MgCl_2$ and 0.5% bovine serum albumin (Sigma, Steinheim, Germany) and incubated overnight at 4 °C in the same solution with alkaline-phosphatase-conjugated anti-digoxigenin-F(ab) fragments (1:5000; Roche Diagnostics GmbH). Afterward, they were washed three times (10 min each) in the same buffer (without antibody), and twice in an alkaline buffer containing 0.1 M Tris–HCl pH 9.5, 0.1 M NaCl, and 5 mM $MgCl_2$. Alkaline phosphatase activity was developed by incubating the sections with 3.3 mg nitroblue tetrazolium and 1.65 mg bromochloroindolyl phosphate (Roche Diagnostics GmbH) diluted in 10 ml of alkaline buffer. The enzymatic reaction was blocked by extensive rinsing in the alkaline buffer containing 1 mM EDTA. The sections were then briefly dipped in 70% and 100% ethanol, air-dried and dipped into Ilford K5 nuclear emulsion (Ilford, Mobberly, Chesire, UK) diluted 1:1 with distilled water. They were exposed in the dark at 4 °C for 6 weeks, and finally developed in Kodak D19 (Kodak, Rochester, NY, USA) for 5 min, and fixed in Ilford Hypam fixer (Ilford).

For film autoradiography, some hybridized sections were exposed to Biomax-MR (Kodak) films for 2–4 weeks at −70 °C with intensifying screens. Consecutive sections were stained with Cresyl Violet for anatomical reference.

Analysis of the results

The average densities of PDE7B mRNA in different brain regions were evaluated semi quantitatively on film autoradiograms with the aid of an image analysis system (MCID M4; Imaging Research, St. Catherines, Ontario, Canada).

Tissue sections were examined in bright- and dark-field in a Wild 420 macroscope (Leica, Heerbrugg, Germany), in a Zeiss Axioplan microscope (Zeiss, Oberkochen, Germany) and in a

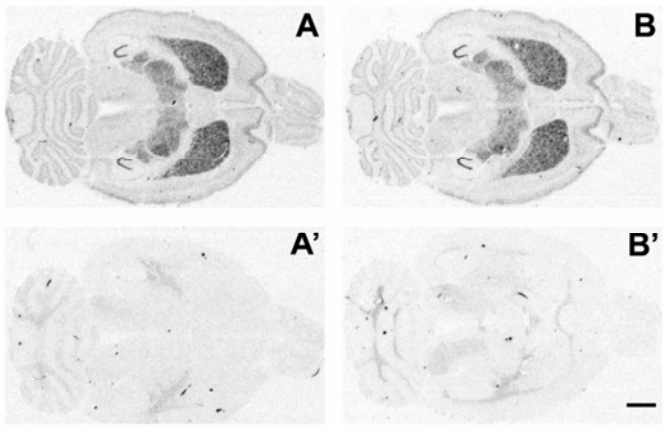

Fig. 1. Specificity controls of the hybridization signal obtained with the two labeled oligonucleotides. Rat horizontal sections were hybridized with ^{33}P-labeled oligonucleotide rPDE7B/1(A) or rPDE7B/2 (B), showing both the same hybridization pattern. No hybridization signal remained after co-hybridizing each labeled oligonucleotide with an excess of the corresponding unlabeled oligonucleotide (A′, B′) Scale bar=2 mm.

Nikon Eclipse E1000 microscope (Nikon, Tokyo, Japan) equipped with bright- and dark-field condensers for transmitted light and with epi-illumination. A Darklite illuminator (Micro Video Instruments, Avon, MA, USA) was used to improve the visualization of autoradiographic silver grains and capture of bright and dark-field images.

Glutamatergic, GABAergic, cholinergic neurons, and also astrocytes and oligodendrocytes, were identified as cellular profiles exhibiting a dark precipitate (alkaline phosphatase reaction product) surrounding or covering the nucleus. PDE7B hybridization signal was considered positive when accumulation of silver grains over the stained cellular profiles was at least two- to three-fold higher than the background levels.

Cell counting was performed manually at the microscope using the analySIS software (Soft Imaging System, Münster, Germany). Only cellular profiles showing abundance of both PDE7B mRNA and the cell type identifier (vGluT1, vGluT2, GAD or ChAT mRNAs) were considered double labeled.

Preparation on figures

Hybridized tissue section images from film autoradiograms were digitalized with an Agfa Duoscan scanner (Agfa Gevaert, Mortsel, Belgium).

Microphotography was performed using a Zeiss Axioplan microscope equipped with a digital camera (DXM1200 F, Nikon) and ACT-1 Nikon Software. Figures were prepared for publication using Adobe Photoshop software (Adobe Software, San Jose, CA, USA). Contrast and brightness of images were the only variables we adjusted digitally. For anatomical reference, sections close to those used were stained with Cresyl Violet.

RESULTS

Controls for specificity of the probes

The specificity of the autoradiographic signal obtained in the *in situ* hybridization histochemistry experiments was con-

Abbreviations used in the figures

Acc	accumbens nucleus
AD	anterodorsal thalamic nucleus
AO	anterior olfactory nucleus
AP	area postrema
Arc	arcuate nucleus
AVVL	anteroventral thalamic nucleus ventrolateral
CA1	field CA1 of the hippocampus
CA3	field CA3 of the hippocampus
CB	cell bridges of the ventral striatum
Cg	cingulate cortex
Cpu	caudate putamen (striatum)
dcl	dense cell layer
DG	dentate gyrus
DLG	dorsal lateral geniculate nucleus
Gr	granular layer of the cerebellum
Hil	hilus of the dentate gyrus
IAD	interanterodorsal thalamic nucleus
ICj	islands of Calleja
ICjM	islands of Calleja major island
LD	laterodorsal thalamic nucleus
LPLR	lateral posterior thalamic nucleus laterorostral
mfl	multiform layer
MGD	medial geniculate nucleus dorsal part
MGM	medial geniculate nucleus medial part
MGV	medial geniculate nucleus ventral part
MHb	medial habenular nucleus
mol	molecular layer of olfactory tubercle
Mol	molecular layer of the cerebellum
PC	Purkinje cell layer of the cerebellum
Pe	periventricular hypothalamic nucleus
PF	prefrontal cortex
Pir	piriform cortex
PMCo	posteromedial cortical amygdaloid group
Po	posterior thalamic nucleus group
RS	retrosplenial cortex
S	subiculum
SFO	subfornical organ
Sol	nucleus of the solitary tract
Str	superior thalamic radiation
Tu	olfactory tubercle
VMHVL	ventromedial nucleus ventrolateral
VML	ventromedial-ventrolateral thalamic nucleus
VP	ventroposterior thalamic nucleus
10	dorsal motor nucleus of vagus

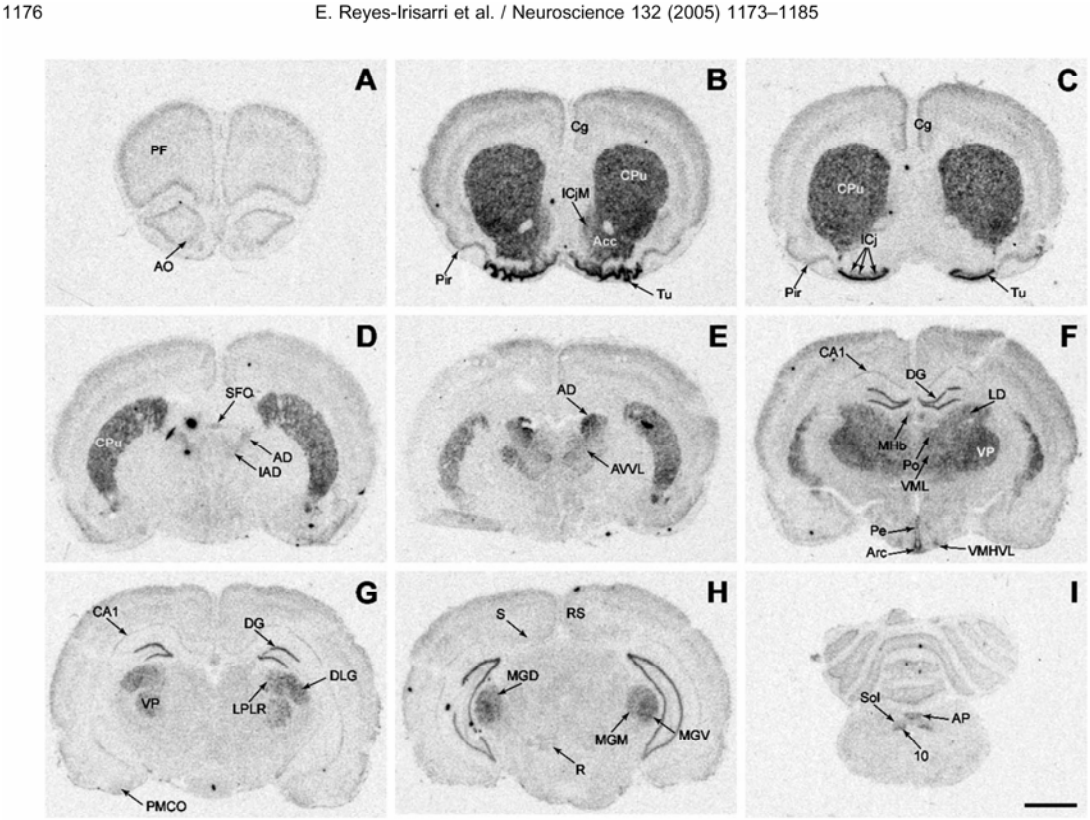

Fig. 2. Regional distribution of PDE7B mRNA in rat brain. Film autoradiograms from rat rostral to caudal sections are presented, showing the hybridization pattern obtained with the ^{33}P-labeled rPDE7B/2 oligonucleotide. Note the intense hybridization signal observed in the olfactory tubercle (Tu), caudate-putamen (CPu), CA1 field and dentate gyrus of the hippocampal formation, and some thalamic nuclei. Scale bar=2 mm.

firmed by performing a series of routine controls (Pompeiano et al., 1992). For each mRNA under study, at least two different oligonucleotide probes complementary to different regions of the same mRNA were used independently as hybridization probes in consecutive sections of the same animal showing identical hybridization patterns (Fig. 1A, B). For a given oligonucleotide probe, addition in the hybridization solution of an excess of the same unlabeled oligonucleotide resulted in the complete abolition of the specific hybridization signal. The remaining autoradiographic signal was considered background (Fig. 1A′, B′). If the unlabeled oligonucleotide included in the hybridization was a different oligonucleotide, then the hybridization signal was not affected (data not shown). The thermal stability of the hybrids was examined by washing at increasing temperatures: a sharp decrease in the hybridization signal was observed at a temperature consistent with the T_m of the hybrids (not shown).

Distribution of PDE7B mRNA

The distribution by *in situ* hybridization histochemistry of PDE7B mRNA transcripts at various coronal levels of the rat brain, illustrated in Fig. 2, showed a selective expression pattern in certain cellular layers and nuclei of the rat brain. Labeled brain nuclei were identified by comparison of the film autoradiograms with Cresyl Violet staining of the hybridized tissues. PDE7B mRNA transcripts were particularly enriched in the olfactory tubercle, striatum, some thalamic nuclei, and the molecular layer of dentate gyrus. Additionally, some layers of the neocortex, piriform cortex, few brainstem nuclei and the Purkinje cells of the cerebellum also presented PDE7B mRNA. A semiquantitative measurement of PDE7B mRNA content in several brain regions is summarized in Table 1.

Cortex

In the prefrontal cortex, PDE7B mRNA (Fig. 2A) was localized in external layers II–III. In other neocortical areas (parietal, temporal and occipital cortices; Fig. 2B–H), hybridization signal was located in the external layers II–III and in deeper layers, V–VI.

Olfactory system

The mRNA coding for PDE7B was weakly expressed in both the olfactory bulb (Fig. 1A, B), and in the anterior olfactory nucleus (Fig. 2A). The highest expression was found in the olfactory tubercle (Figs. 2B, C, 3A), where PDE7B mRNA was present in many intensely labeled

Table 1. Estimated densities of PDE7A mRNA in different regions of the rat brain

Brain area	PDE7A[1]	PDE7B[2]
Cortex		
Parietal cortex	++	++
Frontal cortex	++	++
Cingulate cortex	++	++
Retrospenial cortex	+/++	−/+
Entorhinal cortex	++	+/++
Olfactory system		
Olfactory bulb	+++	+
Anterior olfactory nucleus	++	+
Olfactory tubercle	++	++++
Piriform cortex	+++	++
Islands of Calleja	+/++	++
Islands of Calleja, major island	+/++	+++
Basal ganglia and related areas		
Caudate-putamen	++	+++
Accumbens	−	++/+++
Substantia nigra	++	−
Limbic areas		
Ammon's horn		
CA1 (pyramidal cell layer)	++	+/++
CA2 (pyramidal cell layer)	++/+++	+
CA3 (pyramidal cell layer)	++/+++	+
Dentate gyrus	+++	+++
Subiculum	++	−/+
Pre-,parasubiculum	++	ND
Amygdala	++	+
Lateral septal nucleus	+	−
Medial septal nucleus	+	−
Thalamus and hypothalamus		
Medial habenular nucleus	++/+++	++
Lateral habenular nucleus	+/++	−/+
Anterodorsal thalamic nucleus	ND	+++
Ventroposterior thalamic nuclei	+/++	+++
Laterodorsal thalamic nucleus	+/++	+++
Mediodorsal thalamic nucleus	+/++	+++
Posterior thalamic nucleus group	+	+++
Zona incerta	++	−
Reticular thalamic nucleus	+	−
Ventromedial hypothalamus	+	+
Dorsomedial hypothalamic nucleus	+	−
Arcuate nucleus	+	+
Periventricular hypothalamic nucleus	−	+
Medial geniculate nucleus	+/++	++/+++
Internal capsule	+/++	−
Brainstem		
Red nucleus	++	+
Superior colliculus	+/++	−/+
Pontine nucleus	++/+++	−/+
Ventral tegmental nucleus	++	−
Accessory facial nucleus	++	−
Facial nucleus	+	−
Dorsal cochlear nucleus	+/++	−
Nucleus of the solitary tract	+/++	+/++
Hypoglossal nucleus	++	−
Prepositus hypoglossal nucleus	+/++	−
Cuneate nucleus	++	−
Dorsal motor nucleus of vagus	−	++/+++
Lateral reticular nucleus	+	−
Gracile nucleus	++	−
Inferior olive	+/++	−
Cerebellum		
Molecular layer	−	−
Granular layer	++/+++	+
Purkinje cell layer	+++	++
White matter	−	−
Cerebellar nuclei	+	−/+
Circumventricular organs		
Choroid plexus	++/+++	−
Subfornical organ	−	+
Area postrema	+	++/+++

[1] Labeling intensities for PDE7A mRNA are taken from Miró et al., 2001.

[2] mRNA data are expressed as semiquantitative estimates of hybridization intensity obtained by microdensitometric analysis of film autoradiograms. The levels of hybridization signals are indicated by "+++" very strong; "++" moderate; "+" low; "−/+" very low and "−" not detected.

cells, both in the pyramidal dense cell layer and in cells scattered in the multiform layer (Figs. 2B, C, 3A). By double *in situ* hybridization histochemistry, we have visualized, in the olfactory tubercle, two neuronal populations (GABAergic and cholinergic cells) expressing PDE7B mRNA. Most of the PDE7B mRNA containing cells (79%; see Table 2) of the pyramidal dense cell layer (white grains in Fig. 3C), also co-expressed GAD65 and GAD 67 mRNA, enzyme isoforms responsible of GABA synthesis used as a marker for GABAergic cells (seen as dark precipitate in Fig. 3B, C). Approximately 87% of the cells of the piriform cortex showing moderate to low levels of expression of PDE7B mRNA (Fig. 3A) were glutamatergic cells, visualized as a dark precipitate in Fig. 3D, E due to the hybridization with the oligonucleotide probe complementary to the vesicular GluT1 mRNA. Cholinergic cells were found scattered in the olfactory tubercle, and almost none of them expressed PDE7B mRNA (Fig. 3F, G).

Intermediate levels of PDE7B expression were detected in the compact clusters of granule cells that make up the islands of Calleja (Fig. 2C, 3A) in the multiform cell layer, with very high levels in the island of Calleja magna (Fig. 2B).

Basal ganglia and related areas

Several components of the basal ganglia are among the regions of the rat brain the most enriched in PDE7B mRNA. The nucleus accumbens presented strong hybridization signal (Fig. 2B), with the shell being less intensely labeled than the core. Ventral and lateral to the hybridized cells of the nucleus accumbens, stripes of labeled cells, most likely the striatal cell bridges are observed toward the multiform cell layer of olfactory tubercle (Fig. 3A).

PDE7B mRNA hybridization signal was strong in caudate-putamen (Fig. 2B–F). We attempted to identify the cell type expressing PDE7B mRNA by double *in situ* hybridization histochemistry in this brain area. We have found that up to 74% (Table 2) of PDE7B mRNA-expressing cells, were

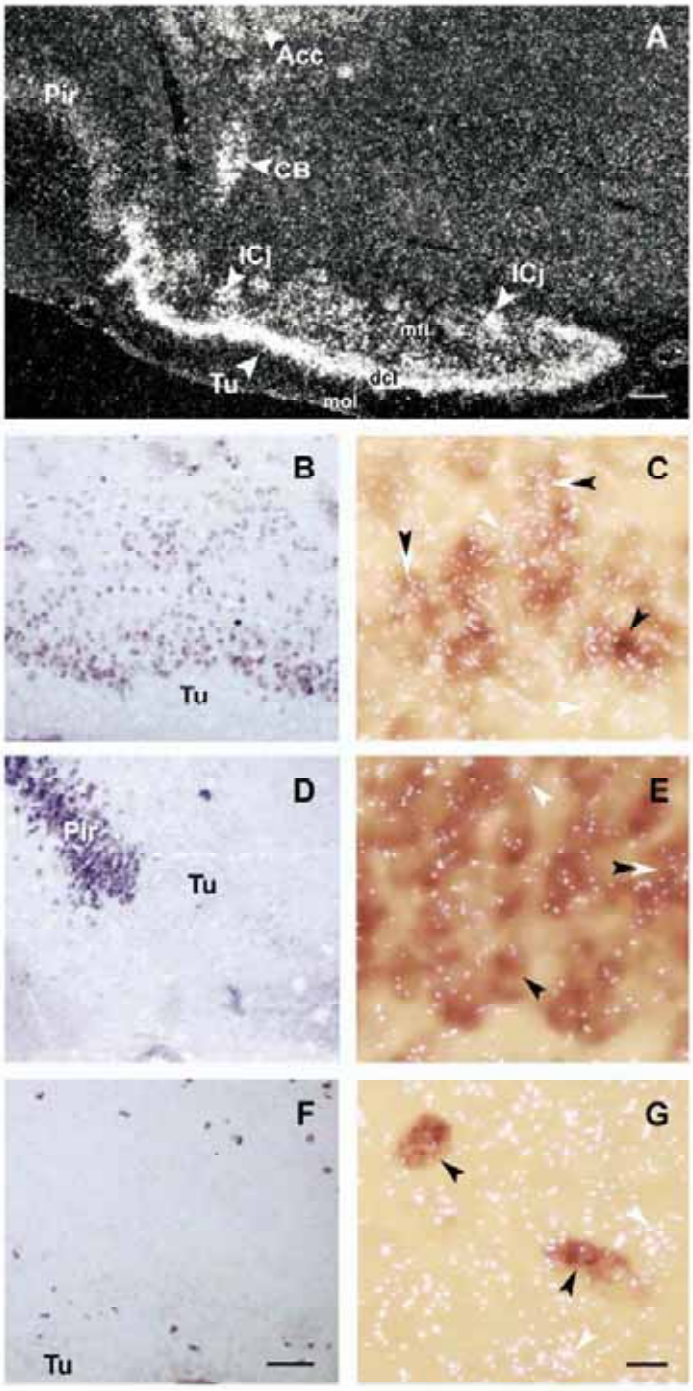

Fig. 3. High magnification dark-field digital photomicrograph of emulsion-dipped section of the ventral accumbens and olfactory tubercle. Autoradiographic grains are seen as bright points and show cells expressing PDE7B mRNA (A). Panels B–G are bright field photomicrographs illustrating the simultaneous detection of two species of mRNAs by double *in situ* hybridization histochemistry using ^{33}P-labeled r7PDEB/2 oligonucleotide (silver grains) and different Dig-labeled oligonucleotides (dark precipitate) for GAD mRNA (B, C), for vGluT1 mRNA (D, E) and for ChAT mRNA (F, G). C, E and G are higher magnification of B, D and F fields, respectively, taken with a Darklite illuminator. Note that photomicrographs were taken in the plane of the autoradiographic grains and therefore cellular staining is slightly out of focus. Scale bars=200 μm A; B, D, F=100 μm; C, E, G=20 μm.

Table 2. Expression of PDE7B isozyme transcripts in glutamatergic (vGluT1 and vGluT2 mRNA positive), GABAergic (GAD mRNA positive) and cholinergic (ChAT mRNA positive) cells

Brain region	vGluT1 mRNA	vGluT2 mRNA	GAD mRNA	ChAT mRNA
Tu	—	—	79.3±6.5	0.3[1]
Pir	87.1±5.1	—	0.5[1]	—
CPu	—	—	74.7±9	0[1]
DG	93.4±1.9	—	0.4[1]	—
Th	76.7±11.3	76±6.7	—	—

[1] Given the low number of GAD and ChAT cells found in those structures only Dig positive cells were counted, in order to estimate the percentage of expression with respect to PDE7B mRNA expressing cells. Data are means of three rats (each individual value is the mean of independent measurements from several fields per area) and represent the percentage of the counted cells expressing the mRNA of PDE7B mRNA in glutamatergic cells independently labeled with vGluT1 and vGluT2 oligonucleotide probes, GABAergic cells which were GAD mRNA-positive and cholinergic expressing the enzyme marker ChAT. The average number of cells counted expressing PDE7B mRNA were: 83±11 cells per each field, in a total of 11 fields (Tu), 57±16 cells per each field, in a total of 17 fields (Pir), 43±16 cells per each field, in a total of 15 fields (CPu), 81±26 cells per each field, in a total of 15 fields (DG), 29±6 cells per each field, in a total of 19 fields (Th).

GABAergic cells, showing low levels of hybridization with GAD 65 and GAD 67 mRNA probes (Fig. 4A, black and white arrow heads). None of the darkest digoxigenin labeled cells expressing GAD 65 and GAD 67 mRNA at high levels was positive for PDE7B mRNA (Fig. 4A, white arrowheads). Cholinergic interneurons, characterized here by the presence of the mRNA coding for ChAT, did not express PDE7B mRNA (Fig. 4B). No hybridization signal for PDE7B mRNA could be detected in cells of globus pallidus (Fig. 2D–F), ventral pallidum (Fig. 2C) and substantia nigra, in both pars reticulata and pars compacta (Fig. 2H).

Limbic areas

Very strong hybridization signals were seen in the granule cell layer of the dentate gyrus (Fig. 2F–H; Fig. 5A), where PDE7B mRNA co-localized with most of the glutamatergic cells (93%; see Table 2; Fig. 5B). The pyramidal cell layer of the CA3 and CA1 fields of the hippocampus presented moderate levels of PDE7B mRNA expression (Fig. 2F–H; Fig. 5A). The subiculum showed very low hybridization levels for PDE7B mRNA (Fig. 2H). Low mRNA expression could be detected in some amygdaloid nuclei (Fig. 2G).

Thalamus and hypothalamus

The mRNA levels of PDE7B isozyme were very high in many thalamic nuclei. Remarkably, strong mRNA densities were seen in anterodorsal thalamic nucleus (Fig. 2E), and in ventroposterior thalamic nucleus (Fig. 2F, G), in both lateral and medial parts. High hybridization levels could be observed in laterodorsal, mediodorsal, posterior, ventromedial and ventrolateral thalamic nuclei (Fig. 2E, F), in dorsolateral geniculate nucleus, lateral posterior thalamic nucleus laterorostral, (Fig. 2G, Fig. 6A, B) and in medial geniculate nucleus dorsal, medial and ventral parts (Fig. 2H). In ventroposterior thalamic (Fig. 6C, E) and dorsolateral geniculate (Fig. 6D, F) nuclei, similar proportions of PDE7B mRNA containing cells (76%) are expressing either vGluT1 (Fig. 6C, D) or vGluT2 (Fig. 6E, F).

In hypothalamus there were a few nuclei containing PDE7B mRNA. Low expression was found in the periventricular hypothalamic nucleus, ventrolateral part of the ventromedial nucleus, and arcuate nucleus (Fig. 2F).

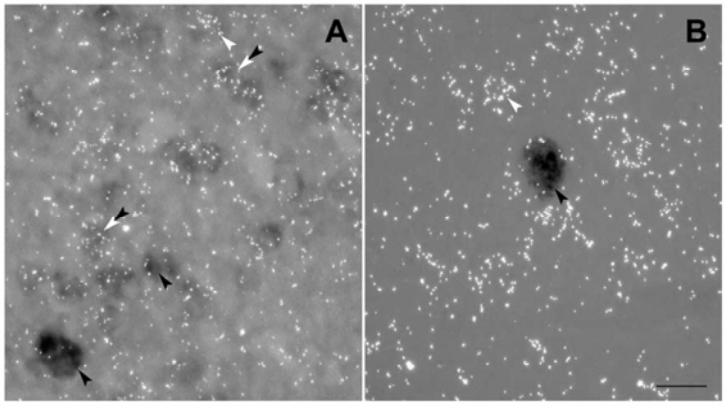

Fig. 4. Cellular localization of PDE7B mRNA (labeled with ^{33}P, white arrowheads) in the cells of the striatum expressing GAD mRNA (dark precipitate in A, black arrowheads) and with ChAT mRNA (dark precipitate in B, black arrowheads). Pictures were taken with a Darklite illuminator. Double-labeled cells expressing both mRNAs are indicated by double black and white arrowheads. Cholinergic cells do not display PDE7B mRNA hybridization signal. Scale bar=20 μm.

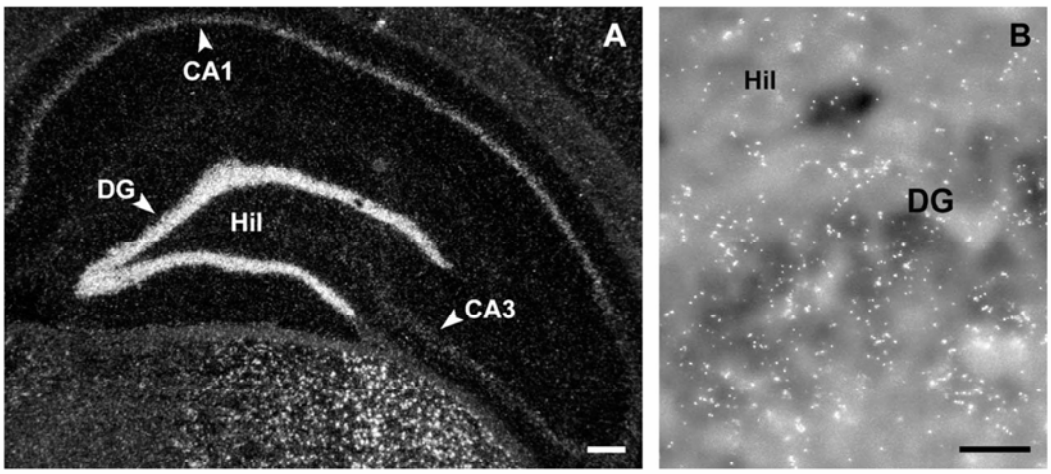

Fig. 5. The expression of PDE7B mRNA in the rat hippocampus (dark-field photomicrograph of emulsion-dipped section in A) is colocalized with glutamatergic cells as shown in the bright field photomicrograph in B. Scale bars=250 μm A; B=20 μm.

Brainstem

The expression of PDE7B mRNA observed in the brainstem nuclei was almost at background levels. Low hybridization signal could be appreciated in the red nucleus (Fig. 2H). We observed moderate hybridization levels in solitary tract and high in the dorsal motor nucleus of the vagus (Fig. 2I).

Cerebellum

In cerebellum, (Fig. 2I) the strongest hybridization signal for PDE7B mRNA was found in the Purkinje cells, much lower levels in the granule cell layer of the cerebellum, whereas PDE7B mRNA was absent in the molecular cell layer (Fig. 7A–C).

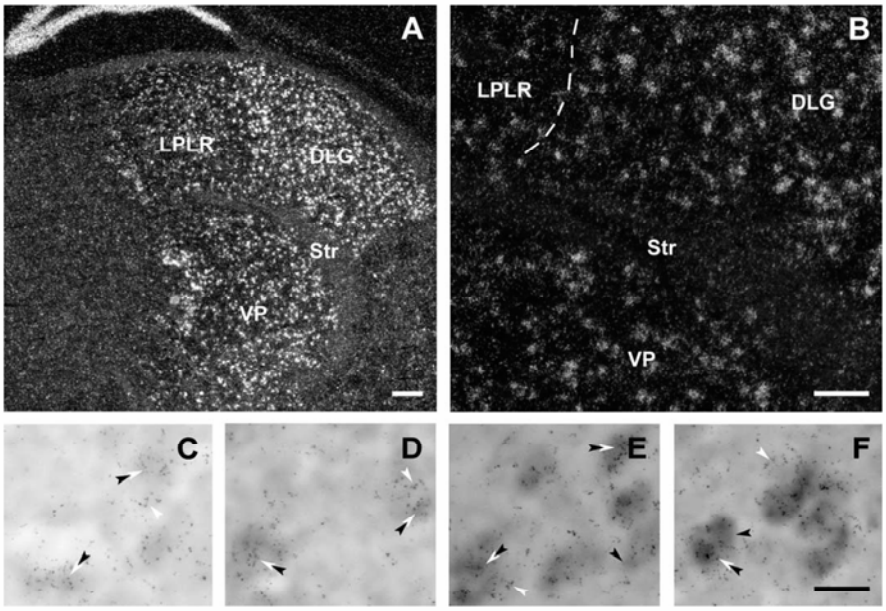

Fig. 6. Cellular distribution of PDE7B mRNA in rat thalamus. A is a dark-field microphotograph of emulsion-dipped section of some thalamic nuclei. B shows a higher magnification of panel A. C–F are bright field photomicrographs illustrating the simultaneous detection by double *in situ* hybridization histochemistry using ^{33}P-labeled rPDE7B/2 oligonucleotide (dark silver grains) and Dig-labeled vGluT1 (C, D) or with Dig-labeled vGluT2 (E, F) oligonucleotides in central thalamic nucleus (C, E) and lateral thalamic nucleus (D, F). Note that both glutamatergic populations of the thalamic nuclei neurons express the mRNA coding for PDE7B isoenzyme. Scale bars=250 μm A; B=100 μm; C–F=20 μm.

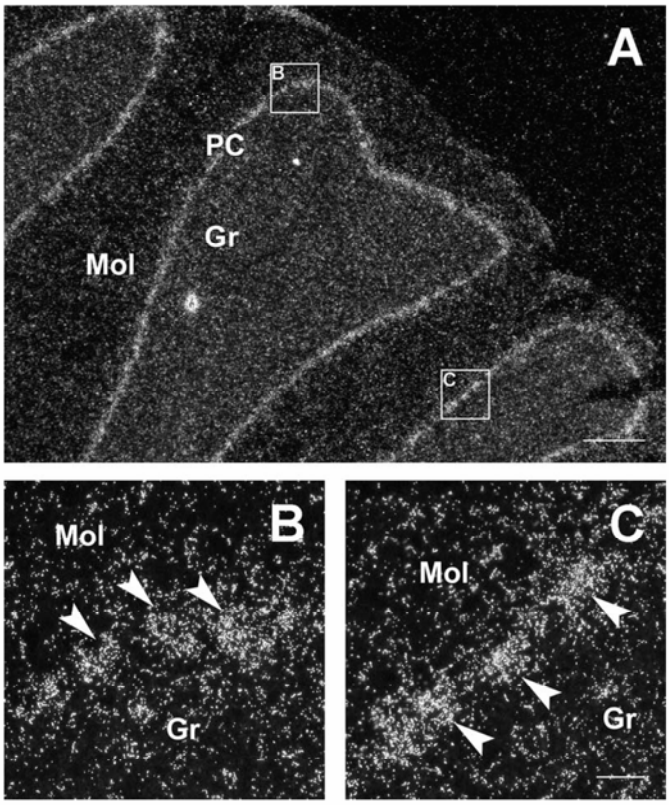

Fig. 7. The expression of PDE7B mRNA in the rat cerebellum. (A–C) Pictures shown are dark field photomicrographs of emulsion-dipped coronal sections. White silver grains show expression of PDE7B mRNA in the Purkinje cell layer (PC). Moderate hybridization levels are seen in granular layer (Gr) and no labeling in molecular layer (Mol). White arrowheads in the high magnifications of the cerebellum in B and C, point to the PC bodies. Scale bars=250 μm A; B=30 μm.

Circumventricular organs

Low hybridization intensities were observed in subfornical organ (Fig. 2D) whereas in area postrema PDE7B mRNA was expressed at high levels (Fig. 2I).

Glial cell population

No hybridization signal for PDE7B mRNA could be detected either in glial cells (identified by the expression of GFAP mRNA) or in oligodendrocytes, expressing MBP mRNA (not shown).

DISCUSSION

We have examined the regional and cellular distribution of PDE7B in the rat brain by using oligonucleotides complementary to the mRNA coding for this isozyme. Our results show that PDE7B mRNA is selectively distributed in the brain and co-expressed in different neurotransmitter-containing cells. To our knowledge, this is the first detailed report of the regional and cellular distribution of PDE7B mRNA in the rat. Previous studies have only partially addressed this issue. The regional and cellular distribution of PDE7B is also different from that of other cAMP-PDEs in the rat brain, suggesting multiple but cell-specific mechanisms of cAMP regulation in the brain.

Some of the results described in the present work are in agreement with those reported by Sasaki et al. (2002). These authors have similarly shown that PDE7B mRNA presented the higher levels of hybridization in the cells of the striatum (both by Northern and *in situ* hybridization). Positive hybridization signal in tissue sections was also described in other regions such as hippocampus, posterior thalamic nuclei, and olfactory nucleus.

When comparing PDE7B mRNA localization to that of PDE7A mRNA (Miró et al., 2001), some overlapping occurs, as summarized in Table 1. PDE7A mRNA expression was found in several cortical areas, in most of the components of the olfactory system, striatum, pyramidal cells of the hippocampus, dentate gyrus, and many thalamic nuclei, regions were PDE7B mRNA was also expressed. In contrast to the expression of PDE7A in many brainstem nuclei, PDE7B mRNA was almost absent there, with the exception of the red nucleus, dorsal motor nucleus of the vagus and nucleus solitarius. This parallel expression of

both components of the PDE7 family in the same brain region could indicate that both enzymes are playing the same function, acting on different regulation pathways in case they were expressed in the same cell.

The areas of the brain showing the highest hybridization levels for PDE7B were striatum, nucleus accumbens, olfactory tubercle and islands of Calleja. PDE7B was completely absent from substantia nigra, globus pallidus and entopeduncular nucleus, in agreement with other authors (Sasaki et al., 2002). The presence of PDE7B mRNA in the granule cells of islands of Calleja could have a connection with the expression of dopamine receptor D3 in these cells (Landwehrmeyer et al., 1993; Sokoloff et al., 1990). It could be an indication of the participation of this isoenzyme in the modulation of the D3 receptor activity and in the function attributed to this group of cells as chemical receptors detecting some factors in the brain and communicating the sensory data to other CNS regions (Millhouse, 1987).

In the striatum PDE7B mRNA was absent from the GABAergic cell population characterized by high GAD65 and GAD67 mRNA content, that could correspond to both interneurons and to large striatonigral projection neurons (Gerfen, 1992; Kita and Kitai, 1988) and also from the cholinergic cells. A great proportion (74%) of the striatal cells expressing PDE7B were GABAergic cells belonging most probably to the medium-spiny projection neurons with intermediate to low hybridization intensities for GAD65 and GAD67 mRNA. This apparent compartmentalization of the expression of PDE7B mRNA in a defined striatal cell population deserves further studies. The striatal medium spiny projection neurons are subdivided into two cellular populations: one expressing substance P/dynorphin, dopamine D1 and adenosine A1 receptors, and projecting to the substantia nigra and entopeduncular nucleus and the other expressing enkephalin, dopamine D2 and adenosine A2A receptors projecting to the globus pallidus, reviewed by Gerfen (1992) and Graybiel (2000). These spiny projection neurons in the striatum are known to use chemically separate channels for their intrastriatal signaling (Lee et al., 1997). Analyzing the cell proportions, it is likely that PDE7B expression is excluded from a particular subset of these medium spiny projection neurons, thus suggesting the possible participation of PDE7B in the regulation of the release of GABA in projecting areas such as substantia nigra, entopeduncular nucleus and globus pallidus. It has been proposed that in substantia nigra, presynaptic D1 receptors can regulate GABA release through a cAMP-mediated mechanism (Radnikow and Misgeld, 1998). Given the importance of the basal ganglia in the movement control and in motor diseases such as Parkinson and Huntington's chorea, it will be of interest to determine the coexpression of PDE7B in the striatal cells with adenylyl cyclase stimulating neurotransmitter receptors located in the striatum such as dopamine D1 (Mengod et al., 1991), serotonin 5-HT_4 (Vilaró et al., 1996) or adenosine A_{2A} (Schiffmann et al., 1991) receptors and also with the dopamine and cAMP-regulated protein 32 kDa phosphoprotein DARPP-32 (Ouimet et al., 1984). The fact that dopamine promotes differentiation of striatal neurons in rat embryonic cultures via stimulation of D1 receptors and the cAMP/PKA signal transduction pathway (Schmidt et al., 1998) underscores the importance of cAMP in striatum. Actually, a transcriptional activation of PDE7B1 through the cAMP pathway by stimulation of D1 receptors in primary striatal cell culture has been very recently described (Sasaki et al., 2004), further supporting the relationship between this isozyme and the dopaminergic signaling system.

When analyzing the modulation of cAMP levels in brain, the presence of several cAMP-specific PDEs has to be taken into account. Thus, striatum presents high expression levels of mRNAs coding for PDE10A (Seeger et al., 2003), PDE4B (Pérez-Torres et al., 2000), PDE9 (Andreeva et al., 2001; van Staveren et al., 2002), PDE1B (Repaske et al., 1993). A detailed study with double *in situ* hybridization histochemistry for PDE7B and the abovementioned striatal enzymes, neuropeptides and receptors, would further contribute to the knowledge of the cAMP involvement in the striatal function. When the K_m values for cAMP of the different PDEs are compared, PDE4 (0.5–4 μM), PDE7 (0.2 μM), PDE8 (0.15 μM), and PDE10A (0.05 μM for cAMP and 3 μM for cGMP) (Soderling et al., 1999; Souness et al., 2000), the first conclusion is that the PDE7 has the higher affinity for cAMP of the single-substrate PDEs, although it should be noticed that the dual-substrate PDE10A has the highest affinity for cAMP. The abovementioned cellular compartmentalization observed for PDE7B in this work, also described for other PDEs, such as, for example, PDE10A (Seeger et al., 2003) could suggest that different isozymes localized in a single cell type could be involved in different physiological processes. The actual affinity of each PDE for the substrate (cAMP), together with the relative abundance of each PDE and the degree of interactions among the different isozymes could be partially controlling the function of medium spiny neurons maintaining the basal levels of cAMP.

The high expression of PDE7B mRNA observed in components of the limbic system points to the possible involvement of this enzyme in processes such as learning, memory, and synaptic plasticity. The pattern of expression of PDE7B mRNA in the brain can be correlated in some areas with the restricted pattern of the expression of different adenylyl cyclases. Thus the high expression of PDE7B in dentate gyrus and also in cerebral cortex is paralleled by the presence of adenylyl cyclase AC1 (Xia et al., 1991), whereas the expression in some hypothalamic nuclei coincides with the presence of AC8 (Cali et al., 1994; Matsuoka et al., 1992), which could suggest that both enzymes will be regulating the intracellular cAMP levels in those particular brain areas. Further studies on colocalization will be necessary.

Sensory relay nuclei of the thalamus such as lateral posterior thalamic, ventroposterior and dorsolateral geniculate nuclei presented a remarkable density of PDE7B mRNA located in glutamatergic cells, expressing either one of the two vGluTs used to identify them (vGluT1 and vGluT2). Some thalamic neurons known to give rise to

thalamocortical and thalamostriatal pathways are glutamatergic (Fujiyama et al., 2001; Ottersen and Storm-Mathisen, 1984). Thus it cannot be ruled out the possible implication of PDE7B in glutamatergic transmission in those brain circuits.

It is interesting to note the expression of PDE7B mRNA in two of the so-called circumventricular organs, subfornical organ located at the rostral tip of the third ventricle and area postrema located around the fourth brain ventricle. Since the subfornical organ is known to be involved in the control of the liquid ingestion responses in the rat (Simpson, 1981), a participation of PDE7B isoenzyme in the drinking behavior could not be excluded. Other cAMP PDEs have been also described to be expressed in the area postrema: PDE7A (Miró et al., 2001), PDE4B and PDE4D (Miró et al., 2002; Pérez-Torres et al., 2000; Takahashi et al., 1999). This circumventral organ is of particular interest since it mediates vomiting and nausea (Borinson and Wang, 1953). The fact that the emetic reflex is triggered in response to receptors acting through cAMP (Carpenter et al., 1988) suggests that cAMP signaling modification in the area postrema could participate in the control of emesis.

There are reports in the literature on the expression of different PDEs in cerebellar Purkinje cells. For example: PDE1B1 (Polli and Kincaid, 1994), PDE5 (Kotera et al., 1997; Shimizu-Albergine et al., 2003), and PDE9 (Andreeva et al., 2001) were described to be expressed in Purkinje cells, PDE1B was detected in a subset of mouse Purkinje cells (Shimizu-Albergine et al., 2003), PDE4 isoenzymes were found in granule cells but not in Purkinje cells (Pérez-Torres et al., 2000) and PDE7A was located in both cerebellar cell populations (Miró et al., 2001), although with higher densities in Purkinje cells. In this work we report on the presence of PDE7B mRNA in both cell populations. It is worth to notice that most of the PDEs found to be expressed in Purkinje cells are cGMP-dependent and that these cells express high levels of soluble guanylate cyclase (Matsuoka et al., 1992). Thus, the presence in the same Purkinje cell of cAMP and cGMP as well as cAMP-dependent PDEs and cGMP-dependent PDEs points to the possibility of cross-talking between these two second messenger systems. This has been already postulated to occur in the contraction of smooth muscle and recently reviewed (Abdel-Latif, 2001), thus supporting our hypothesis.

The knowledge of the protein localization in the brain by using specific antibodies against PDE7B will be an important issue, since the determination of the cellular localization of mRNA coding for this isozyme is not an absolute indication of active enzyme. Determining the precise cellular location of PDE7B and the regulation of its expression and enzymatic activity will be crucial in understanding the physiological role played by this isozyme in the brain.

In summary, we have shown a restricted association of PDE7B mRNA in certain brain areas where this enzyme is expressed in neuronal populations utilizing GABA or glutamate as neurotransmitters. These neurons participate in the control of brain circuits involved in well-characterized functions from movement control (striatum), to high brain functions such as learning, memory and sensory integration (cortex and thalamus). Modulation of brain cAMP levels through inhibition of PDE4 with rolipram has shown the involvement of this second messenger in many brain functions. Because of the selective distribution of PDE7B in the brain, the modulation of this enzyme by pharmacological tools or others could provide new approaches for the treatment of brain diseases

Acknowledgments—This work was supported, by grants from CICYT (SAF1999-0123, SAF2003-02083) and Red CIEN IDIBAPS-ISCIII RTIC C03/06. S.P.-T was a recipient of a fellowship from CIRIT (Generalitat de Catalunya).

REFERENCES

Abdel-Latif AA (2001) Cross talk between cyclic nucleotides and polyphosphoinositide hydrolysis, protein kinases, and contraction in smooth muscle. Exp Biol Med 226:153–163.

Andreeva SG, Dikkes P, Epstein PM, Rosenberg PA (2001) Expression of cGMP-specific phosphodiesterase 9A mRNA in the rat brain. J Neurosci 21:9068–9076.

Bach ME, Barad M, Son H, Zhuo M, Lu YF, Shih R, Mansuy I, Hawkins RD, Kandel ER (1999) Age-related defects in spatial memory are correlated with defects in the late phase of hippocampal long-term potentiation in vitro and are attenuated by drugs that enhance the cAMP signaling pathway. Proc Natl Acad Sci USA 96:5280–5285.

Barad M, Bourtchouladze R, Winder DG, Golan H, Kandel E (1998) Rolipram, a type IV-specific phosphodiesterase inhibitor, facilitates the establishment of long-lasting long-term potentiation and improves memory. Proc Natl Acad Sci USA 95:15020–15025.

Barnes MJ, Cooper N, Davenport RJ, Dyke HJ, Galleway FP, Galvin FC, Gowers L, Haughan AF, Lowe C, Meissner JW, Montana JG, Morgan T, Picken CL, Watson RJ (2001) Synthesis and structure-activity relationships of guanine analogues as phosphodiesterase 7 (PDE7) inhibitors. Bioorg Med Chem Lett 11:1081–1083.

Beavo JA (1995) Cyclic nucleotide phosphodiesterases: functional implications of multiple isoforms. Physiol Rev 75:725–748.

Bloom TJ, Beavo JA (1996) Identification and tissue-specific expression of PDE7 phosphodiesterase splice variants. Proc Natl Acad Sci USA 93:14188–14192.

Borinson HL, Wang SC (1953) Physiology and pharmacology of vomiting. Pharmacol Rev 5:193–230.

Brenner M, Lampel K, Nakatani Y, Mill J, Banner C, Mearow K, Dohadwala M, Lipsky R, Freese E (1990) Characterization of human cDNA and genomic clones for glial fibrillary acidic protein. Mol Brain Res 7:277–286.

Cali JJ, Zwaagstra JC, Mons N, Cooper DM, Krupinski J (1994) Type VIII adenylyl cyclase: a Ca^{2+}/calmodulin-stimulated enzyme expressed in discrete regions of rat brain. J Biol Chem 269:12190–12195.

Carpenter DO, Briggs DB, Knox AP, Strominger N (1988) Excitation of area postrema neurons by transmitters, peptides, and cyclic nucleotides. J Neurophysiol 59:358–369.

Castro A, Abasolo MI, Gil C, Segarra V, Martínez A (2001) CoMFA of benzyl derivatives of 2,1,3-benzo and benzothieno[3,2-alpha]thiadiazine 2,2-dioxides: clues for the design of phosphodiesterase 7 inhibitors. Eur J Med Chem 36:333–338.

Conti M, Jin SL (1999) The molecular biology of cyclic nucleotide phosphodiesterases. Prog Nucleic Acid Res Mol Biol 63:1–38.

Francis SH, Turko IV, Corbin JD (2002) Cyclic nucleotide phosphodiesterases: relating structure and function. Prog Nucleic Acid Res Mol Biol 65:1–52.

Fujiyama F, Furuta T, Kaneko T (2001) Immunocytochemical localization of candidates for vesicular glutamate transporters in the rat cerebral cortex. J Comp Neurol 435:379–387.

Gerfen CR (1992) The neostriatal mosaic: multiple levels of compartmental organization. Trends Neurosci 15:133–139.

Graybiel AM (2000) The basal ganglia. Curr Biol 10:R509–R511.

Hetman JM, Soderling SH, Glavas NA, Beavo JA (2000) Cloning and characterization of PDE7B, a cAMP-specific phosphodiesterase. Proc Natl Acad Sci USA 97:472–476.

Hoffmann R, Abdel'Al S, Engels P (1998) Differential distribution of rat PDE-7 mRNA in embryonic and adult rat brain. Cell Biochem Biophys 28:103–113.

Houslay MD (1998) Adaptation in cyclic AMP signalling processes: a central role for cyclic AMP phosphodiesterases. Semin Cell Dev Biol 9:161–167.

Houslay MD, Milligan G (1997) Tailoring cAMP-signalling responses through isoform multiplicity. Trends Biochem Sci 22:217–224.

Ishii K, Oda Y, Ichikawa T, Deguchi T (1990) Complementary DNAs for choline acetyltransferase from spinal cords of rat and mouse: nucleotide sequences, expression in mammalian cells, and in situ hybridization. Brain Res Mol Brain Res 7:151–159.

Kita H, Kitai ST (1988) Glutamate decarboxylase immunoreactive neurons in rat neostriatum: their morphological types and populations. Brain Res 447:346–352.

Kotera J, Yanaka N, Fujishige K, Imai Y, Akatsuka H, Ishizuka T, Kawashima K, Omori K (1997) Expression of rat cGMP-binding cGMP-specific phosphodiesterase mRNA in Purkinje cell layers during postnatal neuronal development. Eur J Biochem 249:434–442.

Landry M, Holmberg K, Zhang X, Hokfelt T (2000) Effect of axotomy on expression of NPY, galanin, and NPY Y1 and Y2 receptors in dorsal root ganglia and the superior cervical ganglion studied with double-labeling in situ hybridization and immunohistochemistry. Exp Neurol 162:361–384.

Landwehrmeyer B, Mengod G, Palacios JM (1993) Differential visualization of dopamine D2 and D3 receptor sites in rat brain: a comparative study using in situ hybridization histochemistry and ligand binding autoradiography. Eur J Neurosci 5:145–153.

Lee R, Wolda S, Moon E, Esselstyn J, Hertel C, Lerner A (2002) PDE7A is expressed in human B-lymphocytes and is up-regulated by elevation of intracellular cAMP. Cell Signal 14:277–284.

Lee T, Kaneko T, Taki K, Mizuno N (1997) Preprodynorphin-, preproenkephalin-, and preprotachykinin-expressing neurons in the rat neostriatum: an analysis by immunocytochemistry and retrograde tracing. J Comp Neurol 386:229–244.

Li L, Yee C, Beavo JA (1999) CD3- and CD28-dependent induction of PDE7 required for T cell activation. Science 283:848–851.

Martinez A, Castro A, Gil C, Miralpeix M, Segarra V, Domenech T, Beleta J, Palacios JM, Ryder H, Miró X, Bonet C, Casacuberta JM, Azorin F, Pina B, Puigdomenech P (2000) Benzyl derivatives of 2,1,3-benzo- and benzothieno[3,2-a]thiadiazine 2,2-dioxides: first phosphodiesterase 7 inhibitors. J Med Chem 43:683–689.

Matsuoka I, Giuili G, Poyard M, Stengel D, Parma J, Guellaen G, Hanoune J (1992) Localization of adenylyl and guanylyl cyclase in rat brain by in situ hybridization: comparison with calmodulin mRNA distribution. J Neurosci 12:3350–3360.

Mengod G, Vilaró MT, Niznik HB, Sunahara RK, Seeman P, O'Dowd BF, Palacios JM (1991) Visualization of a dopamine D1 receptor mRNA in human and rat brain. Brain Res Mol Brain Res 10:185–191.

Michaeli T, Bloom TJ, Martins T, Loughney K, Ferguson K, Riggs M, Rodgers L, Beavo JA, Wigler M (1993) Isolation and characterization of a previously undetected human cAMP phosphodiesterase by complementation of cAMP phosphodiesterase-deficient *Saccharomyces cerevisiae*. J Biol Chem 268:12925–12932.

Millhouse OE (1987) Granule cells of the olfactory tubercle and the question of the islands of Calleja. J Comp Neurol 265:1–24.

Miró X, Pérez-Torres S, Palacios JM, Puigdomènech P, Mengod G (2001) Differential distribution of cAMP-specific phosphodiesterase 7A mRNA in rat brain and peripheral organs. Synapse 40:201–214.

Miró X, Pérez-Torres S, Puigdomènech P, Palacios JM, Mengod G (2002) Differential distribution of PDE4D splice variant mRNAs in rat brain suggests association with specific pathways and presynaptical localization. Synapse 45:259–269.

Ottersen OP, Storm-Mathisen J (1984) Glutamate- and GABA-containing neurons in the mouse and rat brain, as demonstrated with a new immunocytochemical technique. J Comp Neurol 229:374–392.

Ouimet CC, Miller PE, Hemmings HC Jr, Walaas SI, Greengard P (1984) DARPP-32, a dopamine- and adenosine 3′:5′-monophosphate-regulated phosphoprotein enriched in dopamine-innervated brain regions: III. Immunocytochemical localization. J Neurosci 4:111–124.

Pérez-Torres S, Cortés R, Tolnay M, Probst A, Palacios JM, Mengod G (2003) Alterations on phosphodiesterase type 7 and 8 isozyme mRNA expression in Alzheimer's disease brains examined by in situ hybridization. Exp Neurol 182:322–334.

Pérez-Torres S, Miró X, Palacios JM, Cortés R, Puigdomènech P, Mengod G (2000) Phosphodiesterase type 4 isozymes expression in human brain examined by in situ hybridization histochemistry and [^{3}H]rolipram binding autoradiography: comparison with monkey and rat brain. J Chem Neuroanat 20:349–374.

Pitts WJ, Vaccaro W, Huynh T, Leftheris K, Roberge JY, Barbosa J, Guo J, Brown B, Watson A, Donaldson K, Starling GC, Kiener PA, Poss MA, Dodd JH, Barrish JC (2004) Identification of purine inhibitors of phosphodiesterase 7 (PDE7). Bioorg Med Chem Lett 14:2955–2958.

Polli JW, Kincaid RL (1994) Expression of a calmodulin-dependent phosphodiesterase isoform (PDE1B1) correlates with brain regions having extensive dopaminergic innervation. J Neurosci 14:1251–1261.

Pompeiano M, Palacios JM, Mengod G (1992) Distribution and cellular localization of mRNA coding for 5-HT1A receptor in the rat brain: correlation with receptor binding. J Neurosci 12:440–453.

Radnikow G, Misgeld U (1998) Dopamine D1 receptors facilitate GABAA synaptic currents in the rat substantia nigra pars reticulata. J Neurosci 18:2009–2016.

Repaske DR, Corbin JG, Conti M, Goy MF (1993) A cyclic GMP-stimulated cyclic nucleotide phosphodiesterase gene is highly expressed in the limbic system of the rat brain. Neuroscience 56:673–686.

Sasaki T, Kotera J, Omori K (2002) Novel alternative splice variants of rat phosphodiesterase 7B showing unique tissue-specific expression and phosphorylation. Biochem J 361:211–220.

Sasaki T, Kotera J, Omori K (2004) Transcriptional activation of phosphodiesterase 7B1 by dopamine D1 receptor stimulation through the cyclic AMP/cyclic AMP-dependent protein kinase/cyclic AMP-response element binding protein pathway in primary striatal neurons. J Neurochem 89:474–483.

Sasaki T, Kotera J, Yuasa K, Omori K (2000) Identification of human PDE7B, a cAMP-specific phosphodiesterase. Biochem Biophys Res Commun 271:575–583.

Schiffmann SN, Jacobs O, Vanderhaeghen JJ (1991) Striatal restricted adenosine A2 receptor (RDC8) is expressed by enkephalin but not by substance P neurons: an in situ hybridization histochemistry study. J Neurochem 57:1062–1067.

Schmidt U, Pilgrim C, Beyer C (1998) Differentiative effects of dopamine on striatal neurons involve stimulation of the cAMP/PKA pathway. Mol Cell Neurosci 11:9–18.

Schmitz GG, Walter T, Seibl R, Kessler C (1991) Nonradioactive labeling of oligonucleotides in vitro with the hapten digoxigenin by tailing with terminal transferase. Anal Biochem 192:222–231.

Seeger TF, Bartlett B, Coskran TM, Culp JS, James LC, Krull DL, Lanfear J, Ryan AM, Schmidt CJ, Strick CA, Varghese AH, Williams RD, Wylie PG, Menniti FS (2003) Immunohistochemical localization of PDE10A in the rat brain. Brain Res 985:113–126.

Serrats J, Artigas F, Mengod G, Cortés R (2003) GABAB receptor mRNA in the raphe nuclei: co-expression with serotonin transporter and glutamic acid decarboxylase. J Neurochem 84:743–752.

Shimizu-Albergine M, Rybalkin SD, Rybalkina IG, Feil R, Wolfsgruber W, Hofmann F, Beavo JA (2003) Individual cerebellar Purkinje cells express different cGMP phosphodiesterases (PDEs): in vivo phosphorylation of cGMP-specific PDE (PDE5) as an indicator of cGMP-dependent protein kinase (PKG) activation. J Neurosci 23:6452–6459.

Simpson JB (1981) The circumventricular organs and the central actions of angiotensin. Neuroendocrinology 32:248–256.

Soderling SH, Bayuga SJ, Beavo JA (1999) Isolation and characterization of a dual-substrate phosphodiesterase gene family: PDE10A. Proc Natl Acad Sci USA 96:7071–7076.

Sokoloff P, Giros B, Martres MP, Bouthenet ML, Schwartz JC (1990) Molecular cloning and characterization of a novel dopamine receptor (D3) as a target for neuroleptics. Nature 347:146–151.

Souness JE, Aldous D, Sargent C (2000) Immunosuppressive and anti-inflammatory effects of cyclic AMP phosphodiesterase (PDE) type 4 inhibitors. Immunopharmacology 47:127–162.

Takahashi M, Terwilliger R, Lane C, Mezes PS, Conti M, Duman RS (1999) Chronic antidepressant administration increases the expression of cAMP-specific phosphodiesterase 4A and 4B isoforms. J Neurosci 19:610–618.

Tomiyama M, Palacios JM, Cortés R, Vilaró MT, Mengod G (1997) Distribution of AMPA receptor subunit mRNAs in the human basal ganglia: an in situ hybridization study. Mol Brain Res 46:281–289.

van Staveren WC, Glick J, Markerink-Van Ittersum M, Shimizu M, Beavo JA, Steinbusch HW, de Vente J (2002) Cloning and localization of the cGMP-specific phosphodiesterase type 9 in the rat brain. J Neurocytol 31:729–741.

Vilaró MT, Cortés R, Gerald C, Branchek TA, Palacios JM, Mengod G (1996) Localization of 5-HT4 receptor mRNA in rat brain by in situ hybridization histochemistry. Brain Res Mol Brain Res 43:356–360.

Xia ZG, Refsdal CD, Merchant KM, Dorsa DM, Storm DR (1991) Distribution of mRNA for the calmodulin-sensitive adenylate cyclase in rat brain: expression in areas associated with learning and memory. Neuron 6:431–443.

(Accepted 28 January 2005)
(Available online 11 April 2005)

Trabajo 2:

Expression of the cGMP-specífic phosphodiesterases 2 and 9 in normal and Alzheimer's disease human brains

Elisabet Reyes-Irisarri, Marjanne Markerink-Van Ittersum, Guadalupe Mengod and Jan de Vente.

Publicado en *European Journal of Neuroscience* 25 (2007) 3332-3338

European Journal of Neuroscience, Vol. 25, pp. 3332–3338, 2007 doi:10.1111/j.1460-9568.2007.05589.x

Expression of the cGMP-specific phosphodiesterases 2 and 9 in normal and Alzheimer's disease human brains

Elisabet Reyes-Irisarri,[1] Marjanne Markerink-Van Ittersum,[2] Guadalupe Mengod[1] and Jan de Vente[2]
[1]Department of Neurochemistry, Institut d'Investigacions Biomèdiques de Barcelona, CSIC (IDIBAPS), Barcelona, Spain
[2]Department of Psychiatry and Neuropsychology, Division of Cellular Neuroscience, Maastricht University, European Graduate School of Neuroscience (EURON), 6200 MD Maastricht, the Netherlands

Keywords: Alzheimer's disease, entorhinal cortex, hippocampus, *in-situ* hybridization

Abstract

We studied the mRNA expression of cGMP-hydrolysing phosphodiesterases (PDEs) in selected brain areas of normal elderly people and patients with Alzheimer's disease. Using radioactive *in-situ* hybridization histochemistry we found a widespread distribution of the mRNA for PDE2 and PDE9, whereas no specific hybridization signal was observed for PDE5. We observed PDE2 and PDE9 mRNA in all cortical areas studied (insular cortex, entorhinal cortex and visual cortex), although to a different extent. PDE2 mRNA was high in the claustrum, whereas PDE9 mRNA was moderate. PDE2 and PDE9 mRNAs was present in the putamen. No cGMP-hydrolysing PDE expression was observed in the globus pallidus. PDE2 and PDE9 mRNA was observed in all subareas of the hippocampus; however, there were significant differences in the amount of expression. In the Purkinje and cerebellar granule cells only PDE9 expression was observed. PDE2 and PDE9 mRNA expression was not significantly different in Alzheimer's disease brains.

Introduction

Nitric oxide (NO) is a molecule that readily diffuses through biological membranes and has a signaling function in a large variety of tissues in all animal species (Bicker, 1998; Scholz & Truman, 2000). NO is synthesized by NO synthases. Three different isoforms of this enzyme have been found, i.e. neuronal NO synthase (nNOS) (also NOS-1), inducible NO synthase (or NOS-2) and endothelial NO synthase (or NOS-3) (Alderton *et al.*, 2001). nNOS is expressed throughout the brain and nNOS-containing fibers pervade almost every brain area (Vincent & Kimura, 1992; Southam & Garthwaite, 1993; de Vente *et al.*, 1998; Vincent, 2000). Endothelial NO synthase is found in endothelial cells lining the vasculature of the brain and recently a signaling function towards neurons of NO from endothelial NO synthase has also been described (Garthwaite *et al.*, 2006). nNOS and endothelial NO synthase are calcium/calmodulin-dependent enzymes, whereas inducible NO synthase contains tightly bound calmodulin and is permanently activated (Alderton *et al.*, 2001). There are no data that convincingly demonstrate the expression of inducible NO synthase in the normal brain.

Nitric oxide is a reactive molecule that can react with O_2^-, a normal waste product of mitochondrial respiration, to form peroxynitrite, a toxic molecular species. This fact has led to much attention being given to the role of NO in neurodegeneration (Dawson & Dawson, 1998; Stamler & Hausladen, 1998). However, a role of NO in the pathophysiology of Alzheimer's disease (AD) has not been clearly established. Loss of NO synthase-immunopositive neurons in subfields of the hippocampus was less than for other neuronal cells in the AD hippocampus (Hyman *et al.*, 1992), although the number of NO synthase-containing neuronal fibers was diminished (Rebeck *et al.*, 1993). A decrease (Norris *et al.*, 1996; Thorns *et al.*, 1998) or an increase (Yew *et al.*, 1999) in the number of nNOS-containing cells in the hippocampus has also been reported. An increase in NO synthase/NADPH-diaphorase-containing cells in the substantia innominata of the AD brain has also been reported (Benzing & Mufson, 1995). The data are also not consistent in the frontal cortex of the AD brain (Hyman *et al.*, 1992; Norris *et al.*, 1996; Yew *et al.*, 1999).

The physiological target of NO is the soluble isoform of the enzyme guanylyl cyclase (sGC); activation of the enzyme results in increased synthesis of cGMP (Koesling *et al.*, 2004; Russwurm & Koesling, 2004). This enzyme is also present almost ubiquitously in the brain (Budworth *et al.*, 1999; Gibb & Garthwaite, 2001; Ando *et al.*, 2004; Ding *et al.*, 2004; Pifarre *et al.*, 2007). NO-activated sGC has been demonstrated in almost every brain area of rat and mouse using cGMP immunocytochemistry (Southam & Garthwaite, 1993; de Vente *et al.*, 1998). A decrease in sGC activity has been reported for brain tissues from patients with AD (Bonkale *et al.*, 1995). The concentration of cGMP in the cell is controlled by phosphodiesterases (PDEs) hydrolysing cGMP to 5′-GMP. The PDEs have been classified into 11 subfamilies (Beavo, 1995). Five PDE isoforms are important in hydrolysing cGMP in the brain, i.e. PDE1C, PDE2, PDE5, PDE9 and PDE10 (Conti & Jin, 1999; Beavo & Brunton, 2002). At present, very little is known about the distribution of PDEs in the human brain and these enzymes have not been studied in brain of patients with AD. As the distribution of PDE10 is associated mainly with the substantia nigra–striatal pathways (Fujishige *et al.*, 1999; Seeger *et al.*, 2003) and as very little data are available on PDE1C, we limited our work to study the distribution of PDE2, PDE5 and PDE9 in the brains of patients with AD.

Correspondence: Dr Jan de Vente, as above.
E-mail: j.devente@np.unimaas.nl

Received 15 December 2006, revised 11 April 2007, accepted 13 April 2007

Materials and methods

Specimens

A total of 23 brains, obtained at autopsy, were used for this study. Fourteen subjects had no clinical or morphological evidence of brain pathology and nine were considered clinically and histopathologically as typical cases of AD (Braak III–VI). The characteristics of these individuals are listed in Table 1. Brains were obtained from the Neurological Tissue Bank, University of Barcelona, Hospital Clinic (Barcelona, Spain) and the Department of Neuropathology, Institute of Pathology, Kantonsspital Basel-Universitätskliniken (Basel, Switzerland). All procedures conformed to the European Community Council Directive of November 24, 1986 (86/609/EU).

All brains were obtained at autopsy (post-mortem delay 3–23 h). One cerebral hemisphere was sliced, frozen on dry ice and kept at −20 °C. Tissue sections (14 μm thick) were cut using a microtome-cryostat (Microm HM500 OM, Walldorf, Germany), thaw-mounted onto 3-aminopropyltriethoxysilane (Sigma, St Louis, MO, USA) coated slides and kept at −20 °C until used.

In-situ *hybridization histochemistry*

Antisense and sense ^{33}P-labeled PDE2, PDE5 and PDE9 riboprobes were synthesized by *in-vitro* transcription as described elsewhere (van Staveren *et al.*, 2003). The probes are from the corresponding rat mRNA but share high similarity with the human PDE2, PDE5 and PDE9 mRNA sequences.

Frozen tissue sections were air dried and fixed with 4% paraformaldehyde in 0.1 M phosphate-buffered saline (pH 7.4) for 20 min at room temperature (22 ± 2°C), followed by three short washes with phosphate-buffered saline. Sections were then incubated for 10 min at room temperature with 0.1 M triethanolamine containing 0.25% (v/v) acetic anhydride. Slides were washed twice with 2× sodium saline citrate buffer (SSC) (1× SSC: 150 mM NaCl, 15 mM sodium citrate) for 5 min and thereafter washed at 37 °C with 2× SSC containing 50% (v/v) formamide before the hybridization. Hybridization was performed overnight in a humid chamber at 55 °C under coverslips in 100–200 μL hybridization mix containing 50% (v/v) deionized formamide, 250 μg/mL salmon sperm DNA, 1 mg/mL tRNA, 10% dextran sulfate, 2× SSC, 1× Denhardt's solution and 150–600 ng/mL ^{33}P-labeled RNA probe. After the hybridization, sections were washed at 55 °C in 2× SSC, 1× SSC and 0.1× SSC (all solutions containing 50% formamide, 20 min each). Next, to eliminate single-stranded (unhybridized) probe, the sections were treated with RNAse T1 (2 U/mL, Roche) in 2× SSC containing 1 mM EDTA for 15 min at 37 °C followed by a 20 min wash with 1× SSC at 55 °C. After washing for 10 min with 2× SSC at room temperature, sections were dehydrated through graded ethanol series and air dried. Sections were exposed to Biomax MR (Kodak) films for 10 days and 4 weeks at −70 °C with intensifying screens.

Data analysis

A semiquantitative measure of the relative optical densities was conducted for *in-situ* hybridization studies with the Analytical Imaging Station (AIS®) computerized image analysis system (Imaging Research Inc., St Catharines, Ontario, Canada). We independently measured both sense and antisense hybridized tissues. Final densities were obtained by subtraction of both measurements. The regions analysed were: frontal cortex, subiculum, pyramidal cell layer field 1 of the cornu ammonis (CA1), fields 2/3 of the cornu ammonis (CA2–CA3), dentate gyrus, entorhinal cortex, perirhinal cortex and granular layer of the cerebellum, which were identified with the help of a human atlas (Paxinos, 1990).

We conducted Mann–Whitney tests (PRISM 4, GraphPad Software Inc., San Diego, CA, USA) for the optical densities from the variables examined (PDE2 and PDE9) for each region. The results are expressed as mean ± SEM percentage of control.

TABLE 1. Subject characteristics

Case	Gender	Age (years)	Post-mortem delay	Neuropathology	Immediate cause of death
A	F	85	6 h 30 min	Alzheimer's, Braak VI	Unknown
B	M	77	16 h 30 min	Alzheimer's, Braak V–VI	Unknown
C	M	81	5 h	Alzheimer's, Braak IV	Heart failure
D	F	87	5 h	Alzheimer's, Braak III	Pneumonia
E	F	90	5 h	Alzheimer's, Braak IV	Myocardial infarction
F	F	85	12 h	Alzheimer's, Braak VI	Cardiorespiratory failure
G	M	72	9 h	Alzheimer's, Braak VI	Unknown
H	F	66	6 h 30 min	Alzheimer's, Braak VI	Unknown
I	M	78	18 h	Alzheimer's	Unknown
J	F	70	5 h	Control	Breast cancer. Sudden death
K	M	60	5 h	Control	Myocardial infarction
L	F	75	10 h	Control	Cardiac failure
M	F	76	23 h	Control	Acute breathing failure
N	F	72	6 h	Control	Cardiac embolism
O	F	80	3 h 30 min	Control	Adenocarcinoma
P	M	53	3 h	Control	Myocardial infarction
Q	M	55	7 h	Control	Pneumonia
R	F	65	4 h	Control	Unknown
S	M	51	4 h	Control	Unknown
T	F	79	7 h	Control	Stroke
U	M	52	4 h	Control	Larynx carcinoma
V	M	81	10 h	Control	Colon neoplasia
W	M	73	3 h 30 min	Control	Stroke

M, male; F, female.

Results

Specificity of the hybridization riboprobes

To examine the expression pattern of PDE2, PDE5 and PDE9 mRNAs in some human brain regions we performed *in-situ* hybridization histochemistry experiments using ^{33}P-labeled riboprobes. To control the specificity of the hybridization signal we hybridized adjacent sections with ^{33}P-labeled sense riboprobes. The hybridization signal observed in the control sections was considered as background. With the PDE5 mRNA probe, no hybridization signal was observed on any of the control or AD brains. The reason for this apparent failure to hybridize is not known. It may have been caused by lack of selectivity (unlikely as the homology between rat and human genes is very high) or due to a very low number of PDE5 mRNA copies.

Distribution of phosphodiesterase 2 mRNA in control human brain

The PDE2 mRNA hybridization signal presented a laminar distribution in the insular cortex, being higher in the most external and most internal cellular layers, and absent from layer I (Fig. 1A and F). The expression pattern of PDE2 mRNA is more homogeneous in all cell layers in the entorhinal cortex (Fig. 3A). The expression of PDE2 mRNA in visual cortex presents a different localization, with high densities in layers II, III, V and lower VI (Fig. 5A and F).

High densities could be appreciated in the claustrum and in the putamen (Fig. 2A), whereas PDE2 mRNA was absent from globus pallidus.

The PDE2 mRNA expression in the hippocampal formation (Fig. 3A) was high in the pyramidal cell layer of CA1, CA2 and CA3 fields and in the granule cells of dentate gyrus, and moderate in the hilus, subiculum and presubiculum. Cerebellum and nucleus dentatus showed non-specific hybridization signal (Fig. 4A and C).

Distribution of phosphodiesterase 9 mRNA in control human brain

The PDE9 mRNA hybridization signal was present at moderate levels in the cortical areas examined, i.e. insular (Fig. 1B and G), entorhinal (Fig. 3B) and visual (Fig. 5B and G) cortices.

Moderate densities of PDE9 mRNA could also be seen in the claustrum and in the caudate and putamen (Fig. 2B). This mRNA was not present in globus pallidus.

In the hippocampal formation (Fig. 3B), PDE9 mRNA expression was moderate in the Ammon's fields CA1, CA2 and CA3 and dentate

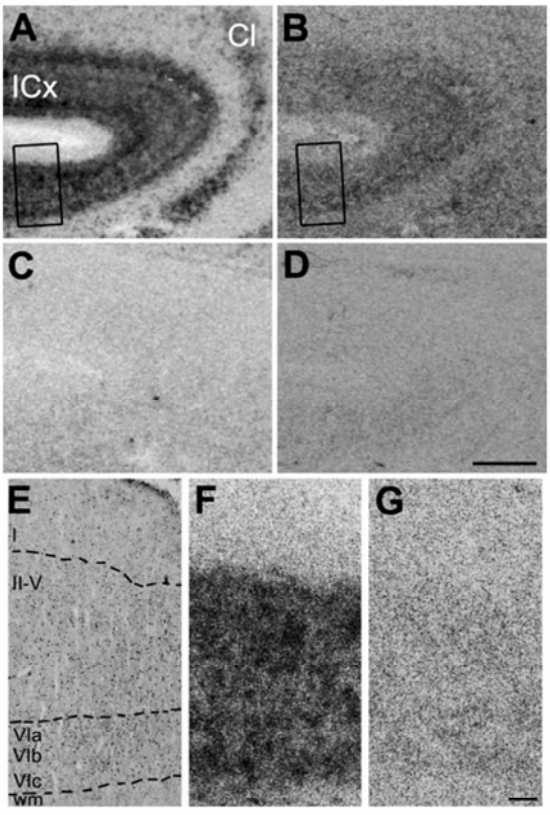

FIG. 1. Distribution of phosphodiesterase (PDE)2 and PDE9 mRNAs in the human insular cortex. Human brain sections were hybridized with antisense riboprobes for PDE2 (A and F) and PDE9 (B and G), and with sense riboprobes for PDE2 (C) and PDE9 (D). (F and G) Higher magnifications of the cortical layer mRNA distribution. (E) Haematoxylin–eosin-stained adjacent section. The different layers are indicated by Roman numerals. PDE2 and PDE9 are specifically expressed in insular cortex (ICx) and claustrum (Cl). Bars: 2 mm (A–D); 200 μm (E–G). wm, white matter.

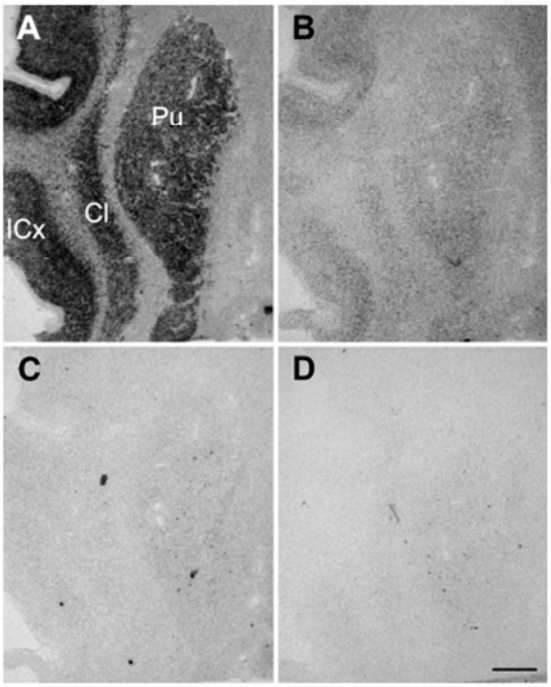

FIG. 2. Distribution of phosphodiesterase (PDE)2 and PDE9 mRNAs in the human basal ganglia at the level of globus pallidus. Human brain sections were hybridized with antisense riboprobes for PDE2 (A) and PDE9 (B), and with sense riboprobes for PDE2 (C) and PDE9 (D). PDE2 is highly and specifically expressed in insular cortex (ICx), claustrum (Cl) and putamen (Pu). PDE9 mRNA expression is localized in the insular cortex, claustrum and putamen. Bar, 3 mm (A–D).

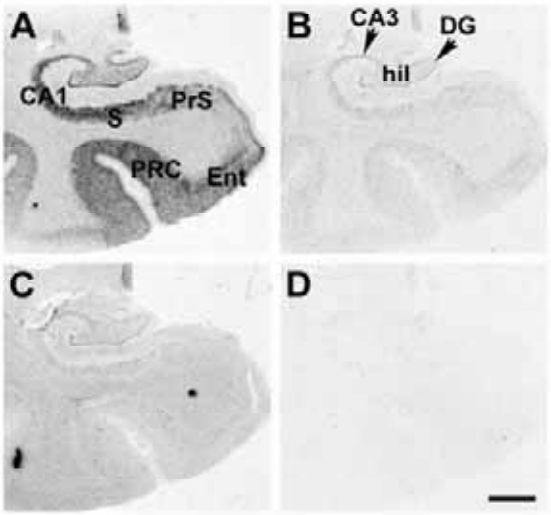

FIG. 3. Distribution of phosphodiesterase (PDE)2 and PDE9 mRNAs in the human hippocampal formation. PDE2 antisense (A) and sense (C) riboprobes, and PDE9 antisense (B) and sense (D) riboprobes. Bar, 4 mm. CA1, field 1 of the cornu ammonis; CA3, field 3 of the cornu ammonis; DG, dentate gyrus; Ent, entorhinal cortex; hil, hilus; PRC, perirhinal cortex; PrS, presubiculum; S, subiculum.

gyrus, and low in the hilus, subiculum, presubiculum and parasubiculum.

Cerebellum was the brain area analysed that showed the higher hybridization levels for PDE9 mRNA especially in the granule cells of the cerebellum, Purkinje cells (Fig. 4B, F and G) and in the nucleus dentatus (Fig. 4B).

Phosphodiesterase 2 and phosphodiesterase 9 mRNA expression in Alzheimer's disease brain

We analysed by microdensitometry the expression of PDE2 and PDE9 mRNAs in a number of brain areas. Some of these are known to show AD pathology. To determine potential factors that could contribute to the interindividual variation of mRNA expression for the mRNAs examined (PDE2 and PDE9), data were analysed for the effects of age and post-mortem delay by simple correlation analyses. No statistically significant correlations with either age or post-mortem delay were found for the mRNAs examined.

The results obtained are presented in Fig. 6. There were no statistically significant differences for the two mRNAs analysed when their expression levels were compared in control and AD brains. However, when looking at the expression of PDE9 mRNA, a general tendency to a decrease in most of the areas analysed was noticed, especially in the perirhinal cortex. Analysis with the Mann–Whitney test did not show any significant changes in this latter region due to the limited number of AD cases ($n = 3$) in this particular area.

Discussion

In this study we report on the comparison of the localization of two PDE isoforms, i.e. PDE2 and PDE9, in the brains of control humans and of patients with AD. For as yet unknown reasons we did not

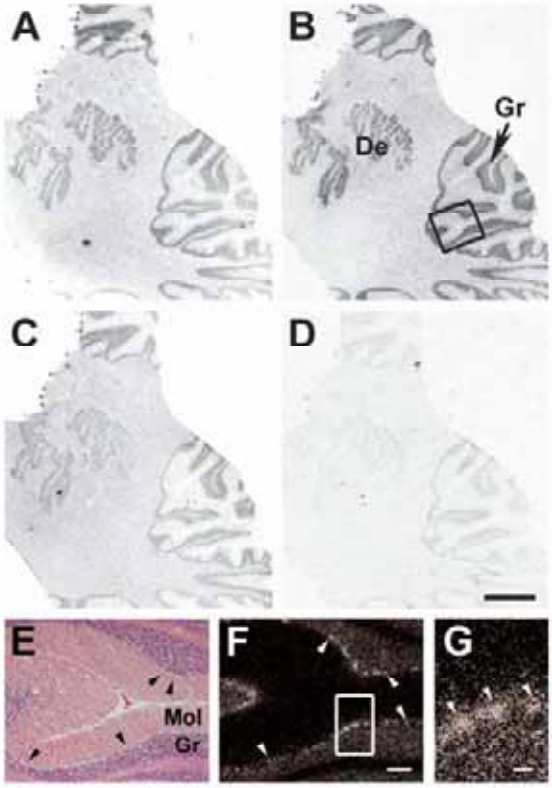

FIG. 4. Phosphodiesterase (*PDE*)2 and *PDE9* mRNA expression in human cerebellum. Digital macrophotographs of film autoradiograms showing the hybridization for PDE2 antisense (A) and sense (C) riboprobes, and for PDE9 antisense (B, F and G) and sense (D) riboprobes. (F and G) Two different magnifications of the Purkinje cell layer expressing PDE9 mRNA. (E) Hematoxylin–eosin-stained adjacent section. Non-specific hybridization signal of PDE2 can be appreciated, whereas PDE9 shows specific hybridization signal in dentate nucleus (De), granular layer of the cerebellum (Gr) and Purkinje cells (arrowheads in E–G). Bars: 4 mm (A–D); 400 μm (E and F); 100 μm (G). Mol, molecular layer of the cerebellum.

observe any hybridization signal using the PDE5 mRNA probe. The main outcomes of this study are firstly that the distributions of mRNA for PDE2 and PDE9 in the human show some differences compared with those found in the rat or mouse, and secondly that there are no significant differences between mRNA expression levels of PDE2 and PDE9 in human control and AD-affected brains.

We have reported previously on the lack of effect of sildenafil (a highly selective PDE5 inhibitor) on NO-stimulated cGMP synthesis in brain slices of old rats (24 months), whereas the response to NO with the combinations of 3-isobutyl-1-methylxanthine or 2-(3,4-dimethoxybenzyl)-7-{(1R)-1-[(1R)-1-hydroxyethyl]-4-phenylbutyl}-5-methyllimidazo[5,1-f][1,2,4]triazin-4(3H)-one (a highly selective PDE2 inhibitor) remained normal. In addition, expression of PDE5 mRNA was significantly decreased, whereas that of PDE2 and PDE9 did not change (Domek-Lopacinska *et al.*, 2005a). This supports our findings on the lack of PDE5 hybridization signal in human brain, which can probably be attributed to very low levels of mRNA expression.

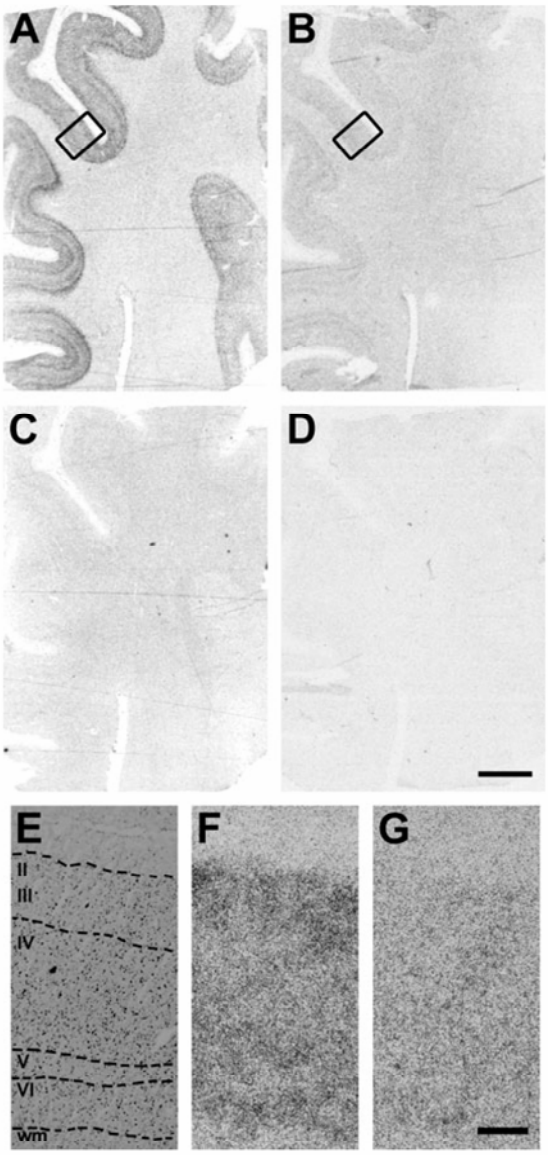

FIG. 5. Distribution of phosphodiesterase (PDE)2 and PDE9 mRNAs in the human visual cortex. Sections were hybridized with ^{33}P-labeled PDE2 antisense (A and F) and sense (C) riboprobes, and PDE9 antisense (B and G) and sense (D) riboprobes. (F and G) Higher magnifications of the cortical layer mRNA distribution. Both mRNAs are expressed in different layers of the cortex. (E) Haematoxylin–eosin-stained adjacent section. The different layers are indicated by Roman numerals. Bars: 4 mm (A–D); 400 μm (E–G). wm, white matter.

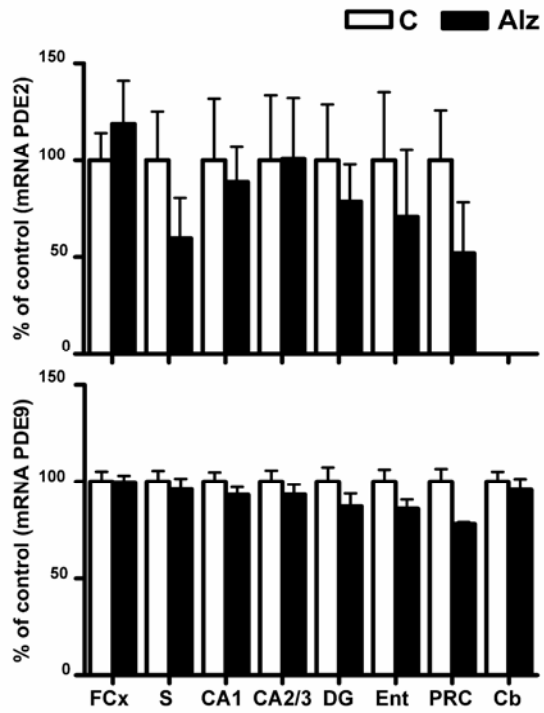

FIG. 6. Bar charts showing phosphodiesterase (PDE)2 and PDE9 mRNA expression in post-mortem brains for control (C) (□, $n = 14$) and Alzheimer's disease (Alz) (■, $n = 9$) in different brain areas. Results are mean values ± SEM expressed as percentage of controls. Mann–Whitney test analysis showed no significant effect of the disease. CA1, field 1 of the cornu ammonis; CA2/3, fields 2/3 of the cornu ammonis; Cb, cerebellum; DG, dentate gyrus; Ent, entorhinal cortex; FCx, frontal cortex; PRC, perirhinal cortex; S, subiculum.

At present, three different isoforms of PDE2 are known, originating by alternative splicing from one gene. Differences between the bovine PDE2A1, rat PDE2A2 and human PDE2A3 are found at the amino terminus (Rosman *et al.*, 1997). For PDE2 *in-situ* hybridization histochemistry we used a construct containing part of the rat PDE2, which was found to be highly expressed in the limbic system of the rat (Repaske *et al.*, 1993). Indeed, we observed strong expression of PDE2 in the hippocampal formation and also the enthorhinal cortex. We were not able to study the other brain areas belonging to the limbic system, as they were not available. A further comparison with the distribution of PDE2 in the rat shows that expression of PDE2 in the human cortex and caudate putamen is similar to that found in the rat. No significant expression was observed in the globus pallidus in both the rat and human. We did not find PDE2 mRNA expression in human cerebellum, in contrast with the rat, where this enzyme is found in cerebellar granule and Purkinje cells (van Staveren *et al.*, 2003).

The structure of PDE9A lacks the cGMP-binding regulatory regions found in PDE2, 5 and 6 (Fisher *et al.*, 1998; Soderling *et al.*, 1998). The sequence identity with the rat and mouse isoform has been reported to be 93% (Guipponi *et al.*, 1998; Soderling *et al.*, 1998), with differences in the N-terminal part. Nevertheless, we obtained a good hybridization signal with the probe derived from the mouse sequence. The expression pattern of human PDE9 mRNA was present at low levels in cortical layers II–VI, which has been similarly reported for the rat brain (Andreeva *et al.*, 2001; van Staveren *et al.*, 2003). These reports also described expression of PDE9 in the caudate putamen and globus pallidus of the rat; however, we did not observe

significant expression in these areas in the human. PDE9 expression in the hippocampal formation and cerebellum was similar in the human and rat.

No significant differences were observed between the expression of PDE2 and PDE9 mRNA in control human brain areas and AD brains. Due to the limited number of AD cases we might characterize these as the result of a pilot experiment. Nevertheless, the observed tendency to a decrease of PDE9 mRNA expression in some areas of AD brains is probably too small to justify physiological consequences for this disease. The involvement of these PDEs in memory process in the normal human or AD brain is not known. It has been shown that the potent PDE2 inhibitor 2-(3,4-dimethoxybenzyl)-7-{(1R)-1-[(1R)-1-hydroxyethyl]-4-phenylbutyl}-5-methyllimidazo[5,1-f][1,2,4]triazin-4(3H)-one improves memory processes in the rat (Boess *et al.*, 2004) and, in a short report, a similar claim has been made for unspecified PDE9A inhibitors (Hendrix, 2005).

Phosphodiesterase mRNA expression represents only one component in the complete signaling pathway from NO synthesis to control of cGMP targets. Therefore, these results do not lead to a conclusion regarding the functioning of this signaling pathway in AD. Nevertheless, a decrease in NO-responsive sGC activity has been reported in the superior temporal cortex of patients with AD (Bonkale *et al.*, 1995). In this study a high concentration (4 mM) of 3-isobutyl-1-methylxanthine was used and the basal sGC activity was not significantly different between controls and AD brain, whereas the activation of sGC by an NO donor was significantly different. This indicates either a difference in the mechanism of activation of sGC or the presence of PDE activity in the AD brain that is not sufficiently inhibited by 3-isobutyl-1-methylxanthine, i.e. PDE9 (Fisher *et al.*, 1998; Soderling *et al.*, 1998). However, we did not observe significant differences in the mRNA expression of PDE9 between controls and AD brains. Therefore, it might be that the decreased reponsiveness of sGC in the AD brain is caused by a decrease in endogenous activators/effectors of sGC (Schmidt *et al.*, 2001; Stasch *et al.*, 2001) or by an increase of an endogenous inhibitor (Mo *et al.*, 2004).

One of the hallmarks of the AD brain is a decreased cholinergic neurotransmission (Cummings *et al.*, 1998; Blusztajn & Berse, 2000). Although there are no data on NO-responsive cGMP-producing structures in the human brain, it has been demonstrated in the rat forebrain that the cholinergic innervation responds to an NO donor with increased cGMP synthesis (de Vente *et al.*, 2000, 2001; Domek-Lopacinska *et al.*, 2005b). It has not yet been established unequivocally what the role of cGMP is in the cholinergic neurons. There are several reports that demonstrate an NO-dependent, stimulatory or facilitatory role of cGMP in acetylcholine release (Guevara-Guzman *et al.*, 1994; Prast *et al.*, 1998; Trabace & Kendrick, 2000; Kraus & Prast, 2001; Buchholzer & Klein, 2002); however, an indirect effect on acetycholine release by NO and/or cGMP cannot yet be excluded (Kendrick *et al.*, 1996; Ikarashi *et al.*, 1998). This topic has been reviewed recently (de Vente, 2004). It was unfortunate that we were not able to study mRNA expression in the cholinergic neurons of the basal forebrain complex, such as the diagonal limb of Broca and the nucleus of Meynert. Cultured fetal cholinergic forebrain neurons from the rat (embryonic day 16) do express PDE2, 5 and 9 mRNAs (J., de Vente, K. Abildayeeva, M. van de Waarenburg, M. Markerink-Van Ittersum, H.W.M. Steinbusch and M. Mulder, unpublished results). As mentioned above, there is a developmental aspect in the expression of the molecular components of the NO-cGMP signaling pathway in the rat basal forebrain. However, there are no data on the human situation. Nevertheless, even if we had been able to investigate this, it would not have enlightened our viewpoint concerning the control of cGMP levels in the cholinergic innervation of the basal forebrain because the distribution of the cGMP-hydrolysing proteins in the neocortex is still not known.

In conclusion, we found widespread localization of PDE2 and PDE9 mRNA in a number of human brain areas. However, we did not observe significant differences in the expression of these enzymes in the brains of controls and patients with AD.

Acknowledgements

The authors are deeply indebted to Dr E. Martínez for the statistical analysis of the data. This work was supported by grants from the ISAO to J.d.V. (grant no. 02506), and Ministerio de Educación y Ciencia, Spain (SAF2003-02083) and Fundació La Marató de TV3 (no. 1017/97) to G.M.

Abbreviations

AD, Alzheimer's disease; CA1, field 1 of the cornu ammonis; CA2/3, fields 2/3 of the cornu ammonis; nNOS, neuronal nitric oxide synthase; NO, nitric oxide; PDE, phosphodiesterase; sGC, soluble guanylyl cyclase; SSC, sodium saline citrate buffer.

References

Alderton, W.K., Cooper, C.E. & Knowles, R.G. (2001) Nitric oxide synthases: structure, function and inhibition. *Biochem. J.*, **357**, 593–615.

Ando, H., Shi, Q., Kusakabe, T., Ohya, T., Suzuki, N. & Urano, A. (2004) Localization of mRNAs encoding alpha and beta subunits of soluble guanylyl cyclase in the brain of rainbow trout: comparison with the distribution of neuronal nitric oxide synthase. *Brain Res.*, **1013**, 13–29.

Andreeva, S.G., Dikkes, P., Epstein, P.M. & Rosenberg, P.A. (2001) Expression of cGMP-specific phosphodiesterase 9A mRNA in the rat brain. *J. Neurosci.*, **21**, 9068–9076.

Beavo, J.A. (1995) Cyclic nucleotide phosphodiesterases: functional implications of multiple isoforms. *Physiol. Rev.*, **75**, 725–748.

Beavo, J.A. & Brunton, L.L. (2002) Cyclic nucleotide research – still expanding after half a century. *Nat. Rev. Mol. Cell Biol.*, **3**, 710–718.

Benzing, W.C. & Mufson, E.J. (1995) Increased number of NADPH-d-positive neurons within the substantia innominata in Alzheimer's disease. *Brain Res.*, **670**, 351–355.

Bicker, G. (1998) NO news from insect brains. *Trends Neurosci.*, **21**, 349–355.

Blusztajn, J.K. & Berse, B. (2000) The cholinergic neuronal phenotype in Alzheimer's disease. *Metab. Brain Dis.*, **15**, 45–64.

Boess, F.G., Hendrix, M., van der Staay, F.J., Erb, C., Schreiber, R., van Staveren, W., de Vente, J., Prickaerts, J., Blokland, A. & Koenig, G. (2004) Inhibition of phosphodiesterase 2 increases neuronal cGMP, synaptic plasticity and memory performance. *Neuropharmacology*, **47**, 1081–1092.

Bonkale, W.L., Winblad, B., Ravid, R. & Cowburn, R.F. (1995) Reduced nitric oxide responsive soluble guanylyl cyclase activity in the superior temporal cortex of patients with Alzheimer's disease. *Neurosci. Lett.*, **187**, 5–8.

Buchholzer, M.L. & Klein, J. (2002) NMDA-induced acetylcholine release in mouse striatum: role of NO synthase isoforms. *J. Neurochem.*, **82**, 1558–1560.

Budworth, J., Meillerais, S., Charles, I. & Powell, K. (1999) Tissue distribution of the human soluble guanylate cyclases. *Biochem. Biophys. Res. Commun.*, **263**, 696–701.

Conti, M. & Jin, S.L. (1999) The molecular biology of cyclic nucleotide phosphodiesterases. *Prog. Nucl. Acid Res. Mol. Biol.*, **63**, 1–38.

Cummings, J.L., Vinters, H.V., Cole, G.M. & Khachaturian, Z.S. (1998) Alzheimer's disease: etiologies, pathophysiology, cognitive reserve, and treatment opportunities. *Neurology*, **51**, S2–S17.

Dawson, V.L. & Dawson, T.M. (1998) Nitric oxide in neurodegeneration. *Prog. Brain Res.*, **118**, 215–229.

Ding, J.D., Burette, A., Nedvetsky, P.I., Schmidt, H.H. & Weinberg, R.J. (2004) Distribution of soluble guanylyl cyclase in the rat brain. *J. Comp. Neurol.*, **472**, 437–448.

Domek-Lopacinska, K., Markerink-Van Ittersum, M., Steinbusch, H.W. & de Vente, J. (2005a) Changes in expression of cGMP selective phosphodiesterases 2, 5 and 9 in the rat brain during aging. *BMC Pharmacol.*, **5** (Suppl. 1), 15.

Domek-Lopacinska, K.W.M., Markerink-Van Ittersum, M., Steinbusch, H.W. & de Vente, J. (2005b) Nitric oxide-induced cGMP synthesis in the cholinergic system during the development and aging of the rat brain. *Brain Res. Dev. Brain Res.*, **158**, 72–81.

Fisher, D.A., Smith, J.F., Pillar, J.S., St Denis, S.H. & Cheng, J.B. (1998) Isolation and characterization of PDE9A, a novel human cGMP-specific phosphodiesterase. *J. Biol. Chem.*, **273**, 15 559–15 564.

Fujishige, K., Kotera, J. & Omori, K. (1999) Striatum- and testis-specific phosphodiesterase PDE10A isolation and characterization of a rat PDE10A [in process citation]. *Eur. J. Biochem.*, **266**, 1118–1127.

Garthwaite, G., Bartus, K., Malcolm, D., Goodwin, D., Kollb-Sielecka, M., Dooldeniya, C. & Garthwaite, J. (2006) Signaling from blood vessels to CNS axons through nitric oxide. *J. Neurosci.*, **26**, 7730–7740.

Gibb, B.J. & Garthwaite, J. (2001) Subunits of the nitric oxide receptor, soluble guanylyl cyclase, expressed in rat brain. *Eur. J. Neurosci.*, **13**, 539–544.

Guevara-Guzman, R., Emson, P.C. & Kendrick, K.M. (1994) Modulation of in vivo striatal transmitter release by nitric oxide and cyclic GMP. *J. Neurochem.*, **62**, 807–810.

Guipponi, M., Scott, H.S., Kudoh, J., Kawasaki, K., Shibuya, K., Shintani, A., Asakawa, S., Chen, H., Lalioti, M.D., Rossier, C., Minoshima, S., Shimizu, N. & Antonarakis, S.E. (1998) Identification and characterization of a novel cyclic nucleotide phosphodiesterase gene (PDE9A) that maps to 21q22.3: alternative splicing of mRNA transcripts, genomic structure and sequence. *Hum. Genet.*, **103**, 386–392.

Hendrix, M. (2005) Selective inhibitors of cGMP phosphodiesterases as procognitive agents. *BMC Pharmacol.*, **5** (Suppl. I), S5.

Hyman, B.T., Marzloff, K., Wenniger, J.J., Dawson, T.M., Bredt, D.S. & Snyder, S.H. (1992) Relative sparing of nitric oxide synthase-containing neurons in the hippocampal formation in Alzheimer's disease. *Ann. Neurol.*, **32**, 818–820.

Ikarashi, Y., Takahashi, A., Ishimaru, H., Shiobara, T. & Maruyama, Y. (1998) The role of nitric oxide in striatal acetylcholine release induced by N-methyl-D-aspartate. *Neurochem. Int.*, **33**, 255–261.

Kendrick, K.M., Guevara-Guzman, R.R.C., Christensen, J., Ostergaard, K. & Emson, P.C. (1996) NMDA and kainate-evoked release of nitric oxide and classical transmitters in the rat striatum: in vivo evidence that nitric oxide may play a neuroprotective role. *Eur. J. Neurosci.*, **8**, 2619–2634.

Koesling, D., Russwurm, M., Mergia, E., Mullershausen, F. & Friebe, A. (2004) Nitric oxide-sensitive guanylyl cyclase: structure and regulation. *Neurochem. Int.*, **45**, 813–819.

Kraus, M.M. & Prast, H. (2001) The nitric oxide system modulates the in vivo release of acetylcholine in the nucleus accumbens induced by stimulation of the hippocampal fornix/fimbria-projection. *Eur. J. Neurosci.*, **14**, 1105–1112.

Mo, E., Amin, H., Bianco, I.H. & Garthwaite, J. (2004) Kinetics of a cellular nitric oxide/cGMP/phosphodiesterase-5 pathway. *J. Biol. Chem.*, **279**, 26 149–26 158.

Norris, P.J., Faull, R.L. & Emson, P.C. (1996) Neuronal nitric oxide synthase (nNOS) mRNA expression and NADPH-diaphorase staining in the frontal cortex, visual cortex and hippocampus of control and Alzheimer's disease brains. *Brain Res. Mol. Brain Res.*, **41**, 36–49.

Paxinos, G. (1990) *The Human Nervous System.* Academic Press, Inc., San Diego.

Pifarre, P., Garcia, A. & Mengod, G. (2007) Species differences in the localization of soluble guanylyl cyclase subunits in monkey and rat brain. *J. Comp. Neurol.*, **500**, 942–957.

Prast, H., Tran, M.H., Fischer, H. & Philippu, A. (1998) Nitric oxide-induced release of acetylcholine in the nucleus accumbens: role of cyclic GMP, glutamate, and GABA. *J. Neurochem.*, **71**, 266–273.

Rebeck, G.W., Marzloff, K. & Hyman, B.T. (1993) The pattern of NADPH-diaphorase staining, a marker of nitric oxide synthase activity, is altered in the perforant pathway terminal zone in Alzheimer's disease. *Neurosci. Lett.*, **152**, 165–168.

Repaske, D.R., Corbin, J.G., Conti, M. & Goy, M.F. (1993) A cyclic GMP-stimulated cyclic nucleotide phosphodiesterase gene is highly expressed in the limbic system of the rat brain. *Neuroscience*, **56**, 673–686.

Rosman, G.J., Martins, T.J., Sonnenburg, W.K., Beavo, J.A., Ferguson, K. & Loughney, K. (1997) Isolation and characterization of human cDNAs encoding a cGMP-stimulated 3′,5′-cyclic nucleotide phosphodiesterase. *Gene*, **191**, 89–95.

Russwurm, M. & Koesling, D. (2004) NO activation of guanylyl cyclase. *EMBO J.*, **23**, 4443–4450.

Schmidt, K., Schrammel, A., Koesling, D. & Mayer, B. (2001) Molecular mechanisms involved in the synergistic activation of soluble guanylyl cyclase by YC-1 and nitric oxide in endothelial cells. *Mol. Pharmacol.*, **59**, 220–224.

Scholz, N.L. & Truman, J.W. (2000) Invertebrate models for studying NO-mediated signaling. In Steinbusch, H.W., de Vente, J. & Vincent, S.R. (Eds), *Handbook of Chemical Neuroanatomy,* Vol. 20. Elsevier, Amsterdam, pp. 417–441.

Seeger, T.F., Bartlett, B., Coskran, T.M., Culp, J.S., James, L.C., Krull, D.L., Lanfear, J., Ryan, A.M., Schmidt, C.J., Strick, C.A., Varghese, A.H., Williams, R.D., Wylie, P.G. & Menniti, F.S. (2003) Immunohistochemical localization of PDE10A in the rat brain. *Brain Res.*, **985**, 113–126.

Soderling, S.H., Bayuga, S.J. & Beavo, J.A. (1998) Identification and characterization of a novel family of cyclic nucleotide phosphodiesterases. *J. Biol. Chem.*, **273**, 15 553–15 558.

Southam, E. & Garthwaite, J. (1993) The nitric oxide-cyclic GMP signalling pathway in rat brain. *Neuropharmacology*, **32**, 1267–1277.

Stamler, J.S. & Hausladen, A. (1998) Oxidative modifications in nitrosative stress. *Nat. Struct. Biol.*, **5**, 247–249.

Stasch, J.P., Becker, E.M., Alonso-Alija, C., Apeler, H., Dembowsky, K., Feurer, A., Gerzer, R., Minuth, T., Perzborn, E., Pleiss, U., Schroder, H., Schroeder, W., Stahl, E., Steinke, W., Straub, A. & Schramm, M. (2001) NO-independent regulatory site on soluble guanylate cyclase. *Nature*, **410**, 212–215.

van Staveren, W.C., Steinbusch, H.W., Markerink-Van Ittersum, M., Repaske, D.R., Goy, M.F., Kotera, J., Omori, K., Beavo, J.A. & de Vente, J. (2003) mRNA expression patterns of the cGMP-hydrolyzing phosphodiesterases types 2, 5, and 9 during development of the rat brain. *J. Comp. Neurol.*, **467**, 566–580.

Thorns, V., Hansen, L. & Masliah, E. (1998) nNOS expressing neurons in the entorhinal cortex and hippocampus are affected in patients with Alzheimer's disease. *Exp. Neurol.*, **150**, 14–20.

Trabace, L. & Kendrick, K.M. (2000) Nitric oxide can differentially modulate striatal neurotransmitter concentrations via soluble guanylate cyclase and peroxynitrite formation. *J. Neurochem.*, **75**, 1664–1674.

de Vente, J. (2004) cGMP: a second messenger for acetylcholine in the brain? *Neurochem. Int.*, **45**, 799–812.

de Vente, J., Hopkins, D.A., Markerink-Van Ittersum, M., Emson, P.C., Schmidt, H.H. & Steinbusch, H.W. (1998) Distribution of nitric oxide synthase and nitric oxide-receptive, cyclic GMP-producing structures in the rat brain. *Neuroscience*, **87**, 207–241.

de Vente, J., Markerink-Van Ittersum, M., van Abeelen, J., Emson, P.C., Axer, H. & Steinbusch, H.W. (2000) NO-mediated cGMP synthesis in cholinergic neurons in the rat forebrain: effects of lesioning dopaminergic or serotonergic pathways on nNOS and cGMP synthesis. *Eur. J. Neurosci.*, **12**, 507–519.

de Vente, J., Markerink-Van Ittersum, M., Axer, H. & Steinbusch, H.W. (2001) Nitric-oxide-induced cGMP synthesis in cholinergic neurons in the rat brain. *Exp. Brain Res.*, **136**, 480–491.

Vincent, S.R. (2000) Histochemistry of the nitric oxyde synthase in the central nervous system. *Handbook of Chemical Neuroanatomy*, Vol. 17. Elsevier, Amsterdam, pp. 19–49.

Vincent, S.R. & Kimura, H. (1992) Histochemical mapping of nitric oxide synthase in the rat brain. *Neuroscience*, **46**, 755–784.

Yew, D.T., Wong, H.W., Li, W.P., Lai, H.W. & W.H. (1999) Nitric oxide synthase neurons in different areas of normal aged and Alzheimer's brains. *Neuroscience*, **89**, 675–686.

Trabajo 3:

Differential expression of PDE4B splice variants in rat brain and their regulation after systemic administration of LPS

Elisabet Reyes-Irisarri, Silvia Pérez-Torres, Xavier Miró, Pere Puigdomènech, Jose M. Palacios y Guadalupe Mengod

Enviado a *Synapse*

DIFFERENTIAL EXPRESSION OF PDE4B SPLICE VARIANTS IN RAT BRAIN AND THEIR REGULATION AFTER SYSTEMIC ADMINISTRATION OF LPS

Elisabet Reyes-Irisarri[1#], Silvia Pérez-Torres[1#], Xavier Miró[2#], Pere Puigdomènech[2], José M. Palacios[3], Guadalupe Mengod[1].

1: Dept. of Neurochemistry, Institut d'Investigacions Biomèdiques de Barcelona, CSIC (IDIBAPS).
2: Dept. of Molecular Genetics, Institut de Biologia Molecular de Barcelona, CSIC.
3: Parc Cientìfic, Universitat de Barcelona.
#: These authors have contributed equally to the work

Running title: PDE4B splice variants expression in rat brain
Correspondence to: Guadalupe Mengod. Dept. of Neurochemistry, Institut d'Investigacions Biomèdiques de Barcelona, CSIC (IDIBAPS). Rosselló, 161, 6ª. 08036 Barcelona, Spain.Tel 34 933 63 83 23, fax 34 933 63 83 01, e-mail: gmlnqr@iibb.csic.es
Keywords: cAMP, inflammation, PDE4B splicing variant, in situ hybridization

The phosphodiesterase 4 (PDE4) family, which specifically hydrolyzes intracellular cAMP, is composed by four isozymes (PDE4A, PDE4B, PDE4C and PDE4D) encoded by different gene loci, and each of them produces several mRNAs by alternative splicing (Houslay et al., 1998). These isozymes and their splice variants are widely expressed in many tissues including the brain (Pérez-Torres et al., 2000; McPhee et al., 2001; Miró et al., 2002; D'Sa et al., 2005). The different knock out mice for PDE4A, PDE4B and PDE4D genes present unique phenotypes, (Jin et al., 1999; Jin and Conti, 2002; Jin et al., 2005), which suggests different functions for these isozymes.

The majority of studies into PDE4 subtype distribution have focused upon inflammatory cells (Engels et al., 1994; Uhlig et al., 1997; Gantner et al., 1998). PDE4A, PDE4B and PDE4D, are found to some extent in different inflammatory cell types, where they could be important regulators of inflammatory processes. Selective inhibitors of PDE4s have been suggested as therapies for the treatment of several human diseases (Menniti et al., 2006), predominantly disorders of the immune and inflammatory systems (Teixeira et al., 1997) or disorders of the central nervous system, such as, depression (O'Donnell and Zhang, 2004) or Alzheimer's disease (McGeer and McGeer, 1995).

The lipopolysaccharide (LPS) is a potent inflammatory agent that has been used to characterize the acute inflammatory process in the brain (Breder et al., 1994; Breder and Saper, 1996). The efficacy of PDE4 inhibitors in inflammation models is remarkable and includes inhibition of LPS-induced increment in serum levels of tumour necrosis factor-α (TNF-α) in liver injury, lung injury, renal failure, mortality (Teixeira et al., 1997; Jin and Conti, 2002) or in a multiple sclerosis mouse model (Moore et al., 2006).

The present study aims to determine the regional distribution in rat brain of the four PDE4B splice variants and to examine the putative involvement of the different PDE4 isozymes in inflammatory processes.

MATERIALS AND METHODS

Animal procedure was performed according to the European Union regulations (O.J. of E.C. L358/1 18/12/1986) and was approved by the Institutional Animal Care and Use Committee. Adult male Wistar rats (200-300 g; Iffa Credo, Lyon, France) used for the neuroanatomical localization of PDE4B splicing variants expression were decapitated and the brain was removed, frozen on dry ice and kept at -20 ºC. LPS treatment was performed as follows: rats were injected intraperitoneally with vehicle or LPS (from Escherichia coli, serotype 055:B5, Sigma, St. Louis, MO, USA; 500 μg/kg of

body weight) diluted in 300 μl of 0.9% sterile saline. Four rats were sacrificed at each of 1, 2, 3 and 4 hr post injection. Eight control rats received an injection of 0.9% sterile saline, and were sacrificed four at each of 2 and 3 hr post injection.

Several oligonucleotides were synthesized for each splicing variant: PDE4B1, bp 383-427, and 506-550, AF202732; PDE4B2 bp 418-462, 520-564, 545-589, L27058; PDE4B3 bp 476-520, 556-600, 616-660, 700-744, U95748; PDE4B4 bp 171-215, 216-260, 264-308, AF202733. COX-2 mRNA oligonucleotides were complementary to bp 1848-1893, NM_017232. The mRNA regions for each PDE4B splice variants were chosen because they share no similarity with each other. Evaluation of the oligonucleotide sequences with basic local alignment search tool of EMBL and GenBank databases indicated that the probes do not present any significant similarity with mRNAs other than their corresponding targets in the rat. The specificity of the autoradiographic signal obtained in the *in situ* hybridization histochemistry experiments was confirmed by performing a series of routine controls (Pompeiano et al., 1992) such as the use of different oligonucleotides for the same mRNA to obtain identical hybridization patterns, competition with the same unlabeled oligonucleotide for the non-specific hybridization signal, determination of the T_m of the hybrids, etc. The procedures followed for the *in situ* hybridization experiments have been published elsewhere (Reyes-Irisarri et al., 2005).

A semiquantitative measure of the optical densities of the autoradiograms was conducted with the MCID4 and AIS^R computerized image analysis systems (Imaging Research Inc, St Catharines, Ontario, Canada). Anatomical brain structures were verified by the examination of cresyl violet-stained sections and identified using a rat brain atlas (Paxinos and Watson, 1998). For each rat, individual values of optical densities in each region were calculated as the mean of 2 adjacent sections in both hemispheres (average of 4 measures per rat and region). The following regions were measured: area postrema, CA fields of the hippocampus, cerebellum, choroid plexus, corpus callosum, dorsal cochlear nucleus, dentate gyrus, hilus, leptomeninges, medial genicular nucleus, medial habenular nucleus, median eminence, organum vasculosum of the lamina terminalis, primary somatosensory cortex, pyramidal tract. Statistical analysis was performed using GraphPad Prism 4 (GraphPad Software Inc, San Diego, CA, USA). Differences among groups per brain region were assessed using the parametric One-way analysis of the variance test followed by the Tuckey's post hoc test for each mRNA. Since no significant statistical difference between the two groups of control rats was observed in any of the regions analyzed, we unified the values as a single control group. Post hoc analysis (Tuckey's test) was performed with a significance set at $p < 0.05$ when the ANOVA indicated that the treatment factor was significant ($p < 0.05$).

RESULTS AND DISCUSSION

mRNA distribution of PDE4B splicing variants in rat brain

We used *in situ* hybridization histochemistry to study the distribution of the four PDE4B splicing variants at various coronal levels of the rat brain (Fig. 1). Table I summarizes our semiquantitative measurements of the content of each mRNA in different brain regions. The splicing variants show a coincident hybridization pattern in several brain areas, such as granular layer of the cerebellum and piriform cortex. In contrast they are differentially expressed in other brain areas, indicating a possible non-redundant role in the regulation of intracellular cAMP levels.

Interestingly, PDE4B1, PDE4B2 and PDE4B3 are detected in the area postrema whereas PDE4B4 is absent (or expressed at very low levels). This area has been implicated as a chemoreceptor trigger zone for emesis (Borinson H.L. and Wang, 1953; Carpenter et al., 1988). The emetic side effects of rolipram are well known, when used as an antidepressant, (Scott et al., 1991). So too are those that other PDE4 inhibitors (such as roflumilast and cilomilast) produce in patients treated with them for asthma or chronic obstructive pulmonary disease (COPD) (Spina, 2003; Chung, 2006). The fact that we found no expression of PDE4B4 mRNA in the rat area postrema

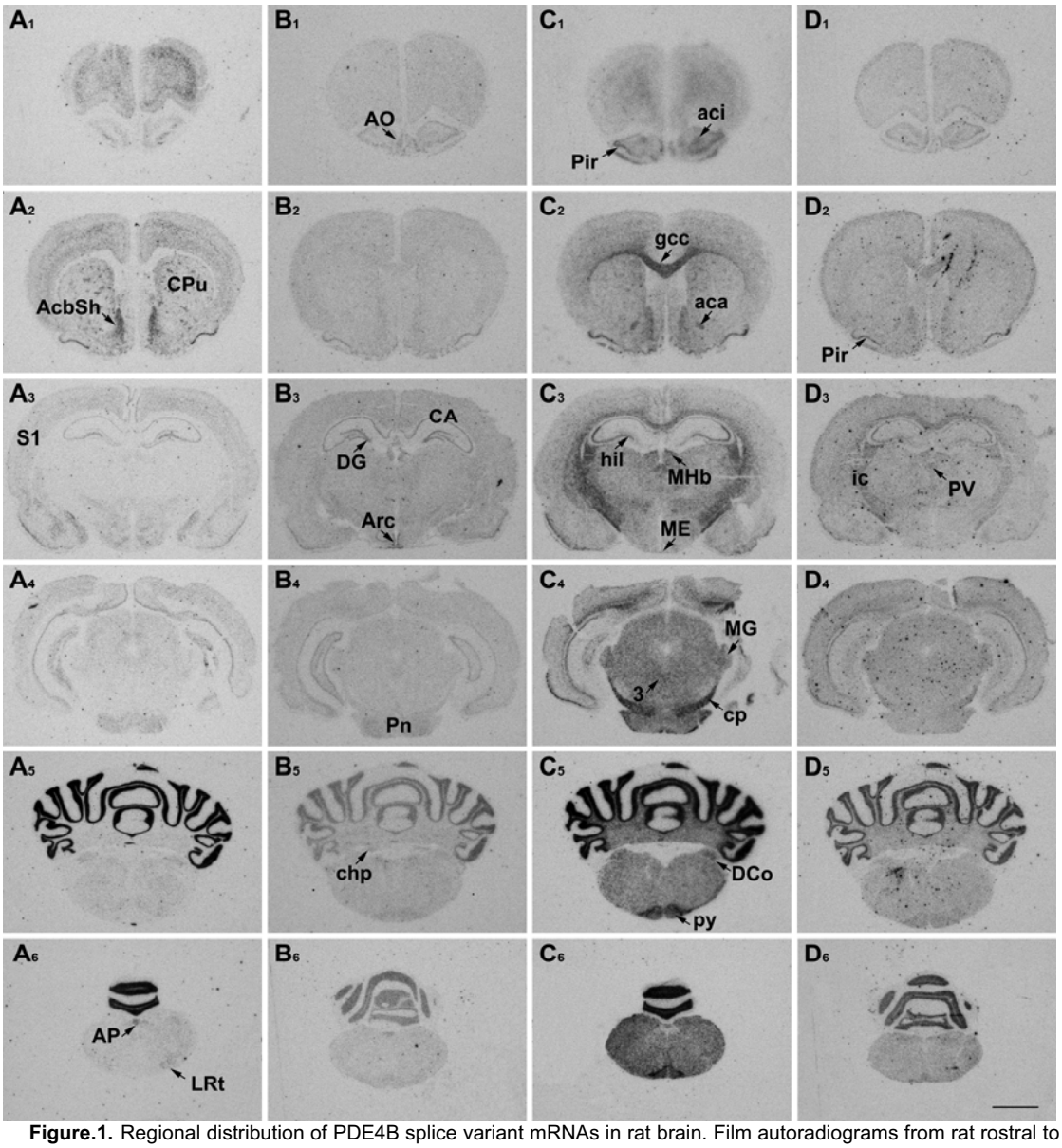

Figure.1. Regional distribution of PDE4B splice variant mRNAs in rat brain. Film autoradiograms from rat rostral to caudal sections are presented, showing the hybridization pattern of PDE4B1 (A_1-A_6), PDE4B2 (B_1-B_6), PDE4B3 (C_1-C_6), and PDE4B4 (D_1-D_6). Note the strong hybridization signal of PDE4B3 in white matter, and the exclusive PDE4B2 expression in dentate gyrus of the hippocampus. aca, anterior commissure, anterior part; AcbSh, accumbens nucleus, shell; aci, anterior commissure, intrabulbar part; AO, anterior olfactory nucleus; AP, area postrema; Arc, arcuate nucleus; CA, Ammon's horn of hippocampus; chp, choroid plexus; cp, cerebral peduncle; CPu, caudate putamen (striatum); DCo, dorsal cochlear nucleus; DG, dentate gyrus; gcc, genu of the corpus callosum; hil, hilus; LRt, lateral reticular nucleus; ME, median eminence; MG: medial genicular nucleus; MHb, medial habenular nucleus; 3, oculomotor nucleus; Pir, piriform cortex; Pn, pontine nuclei; PV, paraventricular thalamic nucleus; py, pyramidal tract; S1: primary somatosensory cortex. Bar =3mm

(even though rodents do not vomit) and that it has been proposed that in humans PDE4B4 exon is unlikely to encode a protein (Shepherd et al., 2003), points to the importance of determining the expression of PDE4 splice variants in this area and other related areas of the human brain. This will help to find candidate targets for specific splicing variant PDE4 inhibitors with no emetic side effects to treat the aforementioned diseases.

In the hippocampal formation all four isoforms are visualized in CA2 and CA3 fields. In the dentate gyrus the only splicing isoform found was PDE4B2. The basic circuitry of the hippocampus is a trisynaptic circuit (Brown and Zador, 1990) where the sensory inputs from the entorhinal cortex

Table I Estimated densities of PDE4B splicing variable mRNAs in different regions of the rat brain

Brain area	PDE4B1	PDE4B2	PDE4B3	PDE4B4
Cortex				
Parietal cortex	+/++	+	+	+/++
Frontal cortex	+/++	+	+	+/++
Cingulate cortex	+/++	+	+	+
Retrospenial cortex	+/++	+	+	+
Entorhinal cortex	+/++	+	+	+
Olfactory system				
Anterior olfactory nucleus	-/+	+/++	+/++	+/++
Olfactory tubercle	+	+/++	+/++	+
Piriform cortex	++/+++	++	++	++
Islands of Calleja	+	+	+	+
Islands of Calleja, major island	+	-/+	+	-/+
Basal ganglia and related areas				
Caudate-Putamen	+/++	-/+	+	-/+
Accumbens				
Core	+	-/+	+/++	-/+
Shell	++	+	+	+
Limbic areas				
Ammon's horn				
CA1 (pyramidal cell layer)	+/++	++	+	+
CA2 (pyramidal cell layer)	+/++	++	++	++
CA3 (pyramidal cell layer)	+/++	++	++	+/++
Dentate gyrus	++	++/+++	-/+	-
Hilus	+	+	+/++	-/+
Subiculum	+	+	+	-/+
Pre, parasubiculum	+	+	+	-/+
Amygdala	+/++	+	+	+
Lateral septal nucleus	+/++	-	-	-/+
Medial septal nucleus	-/+	-/+	+	+
Thalamus and Hypothalamus				
Medial habenular nucleus	-/+	+/++	++	+/++
Lateral habenular nucleus	-/+	+	++	+/++
Paraventricular thalamic nucleus	-	-	++	+/++
Ventroposterior thalamic nuclei	-	+	+	-
Laterodorsal thalamic nucleus	-	+	+	-
Mediodorsal thalamic nucleus	-	+	+	-
Posterior thalamic nucleus group	-	+	+	-
Zona incerta	+	-/+	+/++	-/+
Reticular thalamic nucleus	-	-/+	+	-
Dorsomedial hypothalamus	+/++	-/+	-/+	-
Ventromedial hypothalamus	+/++	+	-/+	-
Arcuate nucleus	-	++/+++	-	-
Periventricular hypothalamic nucleus	-	+	-	-
Medial geniculate nucleus	-/+	+	+/++	+/++
Internal capsule	-	+	++/+++	++
Brainstem				
Superior colliculus	+	+	+/++	+
Oculomotor nucleus	-	+	+/++	-/+
Pontine nucleus	++	++	+/++	+/++
Accessory facial nucleus	-	-/+	+	-/+
Facial nucleus	-/+	-/+	+	+
Dorsal cochlear nucleus	+/++	+	++	+
Nucleus of the solitary tract	+	-/+	-	-/+
Hypoglossal nucleus	-/+	-/+	+	-/+
Cuneate nucleus	-/+	-/+	+/++	-/+
Dorsal motor nucleus of vagus	-/+	-/+	-	-/+
Lateral reticular nucleus	-/+	-/+	+/++	-/+
Gracile nucleus	-	-/+	+/++	-
Inferior olive	-	+	++/+++	+
Cerebellum				
Molecular layer	-	-	-	-
Granular layer	+++	+++	+++	+++
White matter	-	-/+	++	-/+
Cerebellar nuclei	-/+	-/+	+	-
Circumventricular organs				
Choroid plexus	-	-/+	-	-
Area postrema	++	+/++	+/++	-
White matter	-	-	++/+++	+

[1]mRNA data are expressed as semiquantitative estimates of hybridization intensity obtained by microdensitometric analysis of film autoradiograms. The levels of hybridization signals are: "+++" very strong; "++" moderate; "+" weak; "-/+" very weak and "-" not detected. "White matter" includes pyramidal tract, genu corpus callosum, cerebral peduncle and anterior commissure.

arrive at the granule cells of the dentate gyrus, whose main output -via mossy fiber axons- is the pyramidal neurons of CA3, that send their Schaffer collateral axons to

pyramidal neurons of CA1. Some of the synapses of the hippocampus display a remarkable form of plasticity, long-term potentiation (LTP), that could be relevant to the mnemonic functions of this circuitry (Brown et al., 1988), and is a leading candidate for a synaptic mechanism for rapid learning in mammals (Brown and Zador, 1990). This form of plasticity has been studied most in the mossy fiber and in the Schaffer collateral axons. Several authors (Barad et al., 1998; Bach et al., 1999; Rose et al., 2005) suggest that rolipram could enhance hippocampus-dependent memory tasks, and reduce cognitive decline associated with neurodegenerative and psychiatric diseases. These studies together with our finding that PDE4B2 is the only splicing variant expressed in the dentate gyrus, suggest that it could be involved in LTP regulation in the mossy fiber axons. The findings of Ahmed and Frey (2003) that PDE4B3 is involved in the regulation of LTP in the hippocampus, do not invalidate our suggestion, since there are different mechanisms for the two LTP systems: the mossy fibers and the Schaffer collateral inputs. PDE4B3 could be involved in the LTP of Schaffer collateral inputs, (which take place in the CA3 region where all the splicing variants of PDE4B are expressed) and PDE4B2, could be involved in the LTP system of the mossy fibers output, which originates in the dentate gyrus, where PDE4B2 is the only splicing form expressed.

Systemic administration of LPS: effects on the brain.

In order to study the effects of short-term systemic administration of LPS on the expression of PDE4 isozymes in rat brain, we measured the corresponding mRNA levels 1, 2, 3 and 4 hr after LPS treatment in 15 brain areas (including some circumventricular organs) for the 4 splicing variant mRNAs. In order to validate our inflammatory animal model, we analyzed COX-2 mRNA expression in LPS-brains, since COX-2 mRNA is up-regulated in endothelial and perivascular cells of rat and mouse brain blood vessels after LPS administration (Cao et al., 1997). As expected, we found that COX-2 mRNA levels were considerably increased 2 hr after LPS injection in microvasculature and leptomeninges (not shown). When we analyzed the hybridization of the four PDE4B splicing variant mRNAs no significant differences were found between the vehicle and any of the different LPS-treated groups (data not shown) in most of the regions measured, except for choroid plexus, where we found an increment of PDE4B2 mRNA, statistically significant (One-way ANOVA, $F_{4,19}$=4.688, **p*=0.0084), between the vehicle and the 2 and 3 hr groups. In these animal groups mRNA presented a tendency to increase in the rest of the areas.

Upregulation in the expression of several mRNAs has been reported to occur in some of the brain areas we have measured, such as choroid plexus, leptomeninges, and some circumventricular organs (organum vasculosum of the lamina terminalis, median eminence and area postrema) in inflammatory models. Several authors have observed an overexpression of CD14 (Lacroix et al., 1998), TNF-α (Nadeau and Rivest, 1999; Quan et al., 1999), COX-2 (Breder and Saper, 1996; Lacroix and Rivest, 1998) or IKappaB-α (Quan et al., 1997) mRNAs in these regions after a peripheral injection of LPS. The upregulation of PDE4B2 mRNA we observed in the choroid plexus and circumventricular organs after LPS injection could be of interest, given the fact that they may be the sites where communication between peripheral immune system and the brain takes place. The potential role played by PDE4B in inflammation is suported by the work of Conti's group done in PDE4B knockout mice (Jin and Conti, 2002; Jin et al., 2005). Those animals present a decreased responsiveness to LPS in many inflammatory cells: peripheral leukocytes and peritoneal macrophages are not able to secrete TNF-α after LPS stimulation.

To conclude, we have observed a differential distribution of the four splicing variants of PDE4B in the rat brain and a differential regulation for one of the PDE4B splicing variants, PDE4B2, in an inflammatory model. Additional experiments and the development of specific inhibitors for this isoform will help to elucidate its implication in the inflammatory reaction.

ACKNOWLEDGEMENTS

Supported by grants awarded by Fundació La Marató de TV3 (#1017/97), and CICYT (SAF2003-02083, SAF2006-10243). S.P.-T. and X.M. have received a fellowship from CIRIT (Generalitat de Catalunya). We wish to acknowledge technical help from Rocío Martín. We thank Robin Rycroft for English corrections.

REFERENCES

Ahmed T and Frey JU. 2003. Expression of the specific type IV phosphodiesterase gene PDE4B3 during different phases of long-term potentiation in single hippocampal slices of rats in vitro. Neuroscience 117:627-638.

Bach ME, Barad M, Son H, Zhuo M, Lu YF, Shih R, Mansuy I, Hawkins RD, and Kandel ER. 1999. Age-related defects in spatial memory are correlated with defects in the late phase of hippocampal long-term potentiation in vitro and are attenuated by drugs that enhance the cAMP signaling pathway. Proc Natl Acad Sci U S A 96:5280-5285.

Barad M, Bourtchouladze R, Winder DG, Golan H, and Kandel E. 1998. Rolipram, a type IV-specific phosphodiesterase inhibitor, facilitates the establishment of long-lasting long-term potentiation and improves memory. Proc Natl Acad Sci U S A 95:15020-15025.

Borinson H.L. and Wang SC. 1953. Physiology and pharmacology of vomiting. Pharmacol Rev 5:193-230.

Breder CD, Hazuka C, Ghayur T, Klug C, Huginin M, Yasuda K, Teng M, and Saper CB. 1994. Regional induction of tumor necrosis factor alpha expression in the mouse brain after systemic lipopolysaccharide administration. Proc Natl Acad Sci U S A 91:11393-11397.

Breder CD and Saper CB. 1996. Expression of inducible cyclooxygenase mRNA in the mouse brain after systemic administration of bacterial lipopolysaccharide. Brain Res 713:64-69.

Brown TH, Chapman PF, Kairiss EW, and Keenan CL. 1988. Long-term synaptic potentiation. Science 242:724-728.

Brown TH and Zador AM. 1990. Hippocampus. In Gordon M.Shepherd, editor. The Synaptic Organization of the Brain. New York: Oxford University Press. p 346-388.

Cao C, Matsumura K, Yamagata K, and Watanabe Y. 1997. Involvement of cyclooxygenase-2 in LPS-induced fever and regulation of its mRNA by LPS in the rat brain. Am J Physiol 272:R1712-R1725.

Carpenter DO, Briggs DB, Knox AP, and Strominger N. 1988. Excitation of area postrema neurons by transmitters, peptides, and cyclic nucleotides. J Neurophysiol 59:358-369.

Chung KF. 2006. Phosphodiesterase inhibitors in airways disease. Eur J Pharmacol 533:110-117.

D'Sa C, Eisch AJ, Bolger GB, and Duman RS. 2005. Differential expression and regulation of the cAMP-selective phosphodiesterase type 4A splice variants in rat brain by chronic antidepressant administration. Eur J Neurosci 22:1463-1475.

Engels P, Fichtel K, and Lubbert H. 1994. Expression and regulation of human and rat phosphodiesterase type IV isogenes. FEBS Lett 350:291-295.

Gantner F, Gotz C, Gekeler V, Schudt C, Wendel A, and Hatzelmann A. 1998. Phosphodiesterase profile of human B lymphocytes from normal and atopic donors and the effects of PDE inhibition on B cell proliferation. Br J Pharmacol 123:1031-1038.

Houslay MD, Sullivan M, and Bolger GB. 1998. The multienzyme PDE4 cyclic adenosine monophosphate-specific phosphodiesterase family: intracellular targeting, regulation, and selective inhibition by compounds exerting anti-inflammatory and antidepressant actions. Adv Pharmacol 44:225-342.

Jin SL and Conti M. 2002. Induction of the cyclic nucleotide phosphodiesterase PDE4B is essential for LPS-activated TNF-alpha responses. Proc Natl Acad Sci U S A 99:7628-7633.

Jin SL, Lan L, Zoudilova M, and Conti M. 2005. Specific role of phosphodiesterase 4B in lipopolysaccharide-induced signaling in mouse macrophages. J Immunol 175:1523-1531.

Jin SL, Richard FJ, Kuo WP, D'Ercole AJ, and Conti M. 1999. Impaired growth and fertility of cAMP-specific phosphodiesterase PDE4D- deficient mice. Proc Natl Acad Sci U S A 96:11998-12003.

Lacroix S, Feinstein D, and Rivest S. 1998. The bacterial endotoxin lipopolysaccharide has the ability to target the brain in upregulating its membrane CD14 receptor within specific cellular populations. Brain Pathol 8:625-640.

Lacroix S and Rivest S. 1998. Effect of acute systemic inflammatory response and cytokines on the transcription of the genes encoding cyclooxygenase enzymes (COX-1 and COX-2) in the rat brain. J Neurochem 70:452-466.

McGeer PL and McGeer EG. 1995. The inflammatory response system of brain: implications for therapy of Alzheimer and other neurodegenerative diseases. Brain Res Rev 21:195-218.

McPhee I, Cochran S, and Houslay MD. 2001. The novel long PDE4A10 cyclic AMP phosphodiesterase shows a pattern of expression within brain that is distinct from the long PDE4A5 and short PDE4A1 isoforms. Cell Signal 13:911-918.

Menniti FS, Faraci WS, and Schmidt CJ. 2006. Phosphodiesterases in the CNS: targets for drug development. Nat Rev Drug Discov 5:660-670.

Miró X, Pérez-Torres S, Puigdomènech P, Palacios JM, and Mengod G. 2002. Differential distribution of PDE4D splice variant mRNAs in rat brain suggests association with specific pathways and presynaptical localization. Synapse 45:259-269.

Moore CS, Owens T, Earl N, Frenette R, Styhler A, Nicholson DW, Mancini JA, Hebb AL, and Robertson GS. 2006. PERIPHERAL PDE4 INHIBITION PRODUCED BY L-826,141 PREVENTS EXPERIMENTAL AUTOIMMUNE ENCEPHALOMYELITIS. J Pharmacol Exp Ther.

Nadeau S and Rivest S. 1999. Regulation of the gene encoding tumor necrosis factor alpha (TNF-alpha) in the rat brain and pituitary in response in different models of systemic immune challenge. J Neuropathol Exp Neurol 58:61-77.

O'Donnell JM and Zhang HT. 2004. Antidepressant effects of inhibitors of cAMP phosphodiesterase (PDE4). Trends Pharmacol Sci 25:158-163.

Paxinos G and Watson C. 1998. The Rat Brain in stereotaxic coordinates. San Diego: Academic Press.

Pérez-Torres S, Miró X, Palacios JM, Cortés R, Puigdomènech P, and Mengod G. 2000. Phosphodiesterase type 4 isozymes expression in human brain examined by *in situ* hybridization histochemistry and[^{3}H]rolipram binding autoradiography. Comparison with monkey and rat brain. J Chem Neuroanat 20:349-374.

Pompeiano M, Palacios JM, and Mengod G. 1992. Distribution and cellular localization of mRNA coding for 5-HT1A receptor in the rat brain: correlation with receptor binding. J Neurosci 12:440-453.

Quan N, Stern EL, Whiteside MB, and Herkenham M. 1999. Induction of pro-inflammatory cytokine mRNAs in the brain after peripheral injection of subseptic doses of lipopolysaccharide in the rat. J Neuroimmunol 93:72-80.

Quan N, Whiteside M, Kim L, and Herkenham M. 1997. Induction of inhibitory factor kappaBalpha mRNA in the central nervous system after peripheral lipopolysaccharide administration: an in situ hybridization histochemistry study in the rat. Proc Natl Acad Sci U S A 94:10985-10990.

Reyes-Irisarri E, Perez-Torres S, and Mengod G. 2005. Neuronal expression of cAMP-specific phosphodiesterase 7B mRNA in the rat brain. Neuroscience 132:1173-1185.

Rose GM, Hopper A, De Vivo M, and Tehim A. 2005. Phosphodiesterase inhibitors for cognitive enhancement. Curr Pharm Des 11:3329-3334.

Scott AI, Perini AF, Shering PA, and Whalley LJ. 1991. In-patient major depression: is rolipram as effective as amitriptyline? Eur J Clin Pharmacol 40:127-129.

Shepherd M, McSorley T, Olsen AE, Johnston LA, Thomson NC, Baillie GS, Houslay MD, and Bolger GB. 2003. Molecular cloning and subcellular distribution of the novel PDE4B4 cAMP-specific phosphodiesterase isoform. Biochem J 370:429-438.

Spina D. 2003. Phosphodiesterase-4 inhibitors in the treatment of inflammatory lung disease. Drugs 63:2575-2594.

Teixeira MM, Gristwood RW, Cooper N, and Hellewell PG. 1997. Phosphodiesterase (PDE)4 inhibitors: anti-inflammatory drugs of the future? Trends Pharmacol Sci 18:164-171.

Uhlig S, Featherstone RL, Held HD, Nusing R, Schudt C, and Wendel A. 1997. Attenuation by phosphodiesterase inhibitors of lipopolysaccharide-induced thromboxane release and bronchoconstriction in rat lungs. J Pharmacol Exp Ther 283:1453-1459.

Trabajo 4:

Selective induction of cAMP phosphodiesterase PDE4B2 expression in experimental autoimmune encephalomyelitis

Elisabet Reyes-Irisarri, Antonio J Sánchez, Juan Antonio García-Merino y Guadalupe Mengod

En pensa *Journal of Neuropathology and Experimental Neurology*

Selective induction of cAMP phosphodiesterase PDE4B2 expression in experimental autoimmune encephalomyelitis

Elisabet Reyes-Irisarri[1], BSc, Antonio J. Sánchez[2], BSc, Juan Antonio García-Merino[2], MD, PhD, Guadalupe Mengod[1]*, PhD

1: Dept. of Neurochemistry, Instituto de Investigaciones Biomédicas de Barcelona, CSIC (IDIBAPS). c/Rosselló 161, 6ª. E-08036 Barcelona, Spain.

2: Neuroimmunology Unit, Universidad Autónoma de Madrid, Hospital Puerta de Hierro, 28035-Madrid, Spain.

***Author for correspondence:** Guadalupe Mengod, tel 34 933 63 83 23, fax 34 933 63 83 01, e-mail: gmlnqr@iibb.csic.es

Running head title: PDE4B2 upregulation in EAE rat brain

Sources of support: This work was supported by grants awarded by Ministerio de Educación y Ciencia and FEDER Funds (SAF2003-02083, SAF2006-10243).

ABSTRACT

Experimental autoimmune encephalomyelitis in Lewis rats is the most widely used animal model for multiple sclerosis. cAMP has been associated with neuroinflammation. The aim of this study was to investigate the possible involvement of different cAMP-specific phosphodiesterase isoenzymes by analyzing their expression in the brain of EAE rats. We found that in the brain of EAE animals there was a dramatic increase in mRNA expression levels of the PDE4B isozyme detected around blood vessels from the spinal cord to the upper midbrain. There was a single splicing form of the four that are known for PDE4B, PDE4B2, which showed an increase in expression levels. This over-expression is localized around the blood vessels and parenchyma in infiltrating T cells and macrophages/microglia. These results support the role played by the activation of the PDE4B2 gene in the neuroinflammatory process in EAE rats.
Keywords: multiple sclerosis, PDE4, PDE7, neuroinflammation, lymphocytes, microglia.

INTRODUCTION

Multiple sclerosis (MS) is a chronic inflammatory, neurodegenerative disease of the central nervous system, characterized by the destruction of myelin sheaths leading to lesions (1). The composition of the inflammatory infiltrates together with the local expression of cytokines, chemokines and other immune response related molecules suggest that the basis for the inflammatory reaction is an immunological process mediated by T cells. This process disrupts the blood-brain barrier, which leads to the recruitment of other inflammatory cells. In addition, cytokines produced by activated T cells in the lesions induce the activation of effector cells, i.e. macrophages or microglia, which are ultimately responsible for demyelination and tissue damage (2). Experimental autoimmune encephalomyelitis (EAE), the animal model of multiple sclerosis, is an inflammatory disease induced in genetically susceptible animals by active immunization against myelin antigens of the central nervous system (3;4).

The inflammatory process in MS and EAE lesions is dominated by T lymphocytes and activated macrophages/microglia and is associated with the expression of major histocompatibility complex antigens, adhesion molecules and chemokines, which appear to be pivotal in the initiation and propagation of this process [reviewed in (5)]. In addition to T cells, macrophages and activated microglia have been found in areas with active tissue injury, attached to

degenerating myelin sheaths and axons (6;7).

An increase in intracellular cAMP levels is usually accompanied by an inhibition of certain functions of different types of cells involved in the immune response (8;9). Intracellular levels of cAMP are regulated by adenylyl cyclases and cyclic nucleotide 3', 5'-phosphodiesterases (PDEs). Four different PDE4 genes (PDE4A, 4B, 4C and 4D) and two PDE7 genes (PDE7A and 7B) have been identified in rats and humans (10). The mRNAs coding for the PDE4 isoenzyme mRNAs (11;12) and for PDE7 and PDE8 (11;13-15) have been found in the brain of rats, monkeys and humans. PDE4 isozymes are highly expressed in different immune and inflammatory cells, where they may act as important regulators of inflammatory processes (16;17), moreover their expression is differentially modulated in LPS treated rats (Reyes-Irisarri, unpublished) and mice (18-20).

Treatment with rolipram or other PDE4 inhibitors prevents or reduces the pathological process in EAE rats (21;22) and mice (23). Several therapeutic strategies involving PDE4 inhibition have been proposed for MS treatment (24-26).

The possible involvement of cAMP through PDEs in inflammation prompted us to analyze the expression of PDE4 and PDE7 isoenzymes as well as the four mRNA splice variants of PDE4B in the brain of EAE rats.

MATERIALS AND METHODS

Induction of EAE and clinical evaluation

EAE was induced in Lewis rats (Charles River, France) as described elsewhere (27). Briefly, an inoculum containing 50 µg of guinea pig myelin basic protein (gp-MBP) (Sigma-Aldrich Chemie Gmbh, Steinheim, Germany) and 500 µg of *M. tuberculosis* (strain H37Ra, Difco, Detroit, MI) in incomplete Freund's adjuvant (Difco) was injected subcutaneously into the hind footpads. Control rats were injected with *M. tuberculosis* and incomplete Freund's adjuvant in the same way. Rats were examined daily for the presence of neurological signs using the following scale: 0 = no EAE; 1 = partial loss of tail tonicity; 2 = loss of tail tonicity; 3 = unsteady gait and mild paraparesis; 4 = hind-limb paralysis; and 5 = death. Grades 3 and 4 were often accompanied by urinary and fecal incontinence. Animal procedures were performed according to European Union guidelines (86/609/EU) for the use of laboratory animals.

Tissue preparation

The rats were killed by decapitation 10 days and 13 days after the inoculum. The brains were frozen on dry ice and stored at -20ºC. Tissue sections, 14 µm thick, were cut on a microtome-cryostat (Microm HM500 OM, Walldorf, Germany), thaw-mounted onto APTS (3-aminopropyltriethoxysilane; Sigma-Aldrich Chemie Gmbh) coated slides, and stored at -20ºC until use.

Hybridization probes

The oligonucleotides used to detect the mRNAs coding for different PDEs, TCRβ (T cell receptor active beta-chain C-region, T cell marker) and PAFR (platelet activated factor receptor, microglia marker) are shown in Table 1. They were all synthesized and HPLC purified by Isogen Bioscience BV (Maarsden, The Netherlands). The hybridization conditions to detect all mRNAs have been described elsewhere (11;12;15).

The mRNA regions for each mRNA analyzed were chosen because they share no similarity with each other. Evaluation of the oligonucleotide sequences with basic local alignment search tool of EMBL and GenBank databases indicated that the probes do not present any significant similarity with mRNAs other than their corresponding targets in the rat. The specificity of the autoradiographic signal obtained in the *in situ* hybridization histochemistry experiments was confirmed by performing a series of routine controls (28) such as the use of different oligonucleotides for the same mRNA to obtain identical hybridization patterns, competition with the same unlabeled oligonucleotide for the non-specific hybridization signal, determination of the T_m of the hybrids, etc. The probes used to visualize the four PDE4B mRNA splicing variants have been described elsewhere (Reyes-Irisarri and Mengod, unpublished work).

Oligonucleotides for each PDE were labeled at their 3'-end using [α-^{33}P]dATP (3000 Ci/mmol, New England Nuclear, Boston, MA, USA) and terminal

deoxynucleotidyltransferase (TdT, Calbiochem, San Diego, CA, USA), obtaining a final specific activity of 0.9-2.7 x 10^4 Ci/mmol. They were purified using ProbeQuant G-50 Micro Columns (GE Healthcare, Buckinghamshire, UK) (15). PAFR and TCRβ oligonucleotides were non-radioactively labeled with recombinant terminal deoxynucleotidyltransferase (TdTrec, Roche Diagnostics GmbH, Penzberg, Germany) and DIG-11-dUTP (Boehringer Mannheim, Germany) according to a previously described procedure (29).

In situ *hybridization histochemistry procedure*

The protocols for single- and double-label *in situ* hybridization histochemistry were based on previously described procedures (30;31) and are published elsewhere (15;32). Frozen tissue sections were brought to room temperature, fixed for 20 min at 4ºC in 4% paraformaldehyde in phosphate-buffered saline (1x PBS: 8 mM Na_2HPO_4, 1.4 mM KH_2PO_4, 136 mM NaCl, 2.6 mM KCl), washed for 5 min in 3x PBS at room temperature, twice for 5 min each in 1x PBS, and incubated for 2 min at 20ºC in a solution of predigested pronase (Calbiochem) at a final concentration of 24 U/ml in 50 mM Tris-HCl pH 7.5, 5 mM EDTA. The enzymatic activity was stopped by immersion for 30 sec in 2mg/ml glycine in 1x PBS. Tissues were finally rinsed in 1x PBS and dehydrated through a graded ethanol series. For hybridization, radioactively-labeled and non-radioactively labeled probes were diluted in a solution containing 50% formamide, 4x SSC (1x SSC: 150 mM NaCl, 15 mM sodium citrate), 1x Denhardt's solution (0.02% Ficoll, 0.02% polyvinylpyrrolidone, 0.02% bovine serum albumin), 10% dextran sulfate, 1% sarkosyl, 20 mM phosphate buffer pH 7.0, 250 µg/ml yeast tRNA and 500 µg/ml salmon sperm DNA. The final concentrations of radioactive and DIG-labeled probes in the hybridization buffer were in the same range (approximately 1.5 nM). Tissue sections were covered with hybridization solution containing the labeled probe/s, overlaid with Nescofilm coverslips (Bando Chemical Ind, Kobe, Japan) and incubated overnight at 42ºC in humid boxes. Sections were washed four times (45 min each) in 0.6M NaCl, 10mM Tris-HCl pH 7.5 at 60ºC, and once in the same buffer at room temperature for 10 min.

Development of radioactive and non-radioactive hybridization signal

Hybridized sections were treated as described in (31). After washing, the slides were immersed for 30 min in a buffer containing 0.1 M Tris-HCl pH 7.5, 1 M NaCl, 2 mM $MgCl_2$ and 0.5% bovine serum albumin (Sigma-Aldrich Chemie Gmbh) and incubated overnight at 4ºC in the same solution with alkaline phosphate-conjugated anti-digoxigenin-Fab fragments (1:5000; Boehringer Mannheim). They were then washed three times (10 min each) in the same buffer (without antibody), and twice in an alkaline buffer containing 0.1 M Tris-HCl pH 9.5, 0.1 M NaCl, and 5 mM $MgCl_2$. Alkaline phosphatase activity was developed by incubating the sections with 3.3 mg nitroblue tetrazolium and 1.65 mg bromochloroindolyl phosphate (Gibco BRL, Gaithersburg, MD, USA) diluted in 10 ml of alkaline buffer. The enzymatic reaction was blocked by extensive rinsing in the alkaline buffer containing 1 mM EDTA. The sections were then briefly dipped in 70% and 100% ethanol, air-dried and dipped into Ilford K5 nuclear emulsion (Ilford, Mobberly, Chesire, UK) diluted 1:1 with distilled water. They were exposed in the dark at 4°C for 4-6 weeks and finally developed in Kodak D19 (Kodak, Rochester, NY, USA) for 5 min and fixed in Ilford Hypam fixer (Ilford).

For film autoradiography, some hybridized sections were exposed to Biomax-MR (Kodak) films for 2-4 weeks at -70ºC with intensifying screens.

Immunohistochemistry

Adjacent sections to those used for *in situ* hybridization histochemistry were also examined by immunohistochemistry. To detect the different cell types, the following primary antibodies were used: mouse anti-rat CD11b (1:100, Serotec, Oxford, UK) for microglia; mouse anti-neuronal-specific nuclear protein (NeuN, 1:1000, Chemicon International, CA, USA) for neuronal cell population; rabbit anti-human CD3 (1:100, Dako Cytomation, Glostrup, Denmark) for T cells.

The secondary antibodies used were: biotinylated anti-mouse IgG (H+L) (1:300, Vector Laboratories, CA, USA) and biotinylated anti-rabbit IgG (H+L) (1:100, Vector Laboratories).

The sections were fixed for 20 min at 4ºC in 4% PFA, rinsed in 1xPBS for 5 min and incubated for 15 min in a solution containing 0.3% H_2O_2 (Sigma-Aldrich Chemie Gmbh) in 1xPBS. After rinsing in 1xPBS for 5 min, preincubation and incubation with primary and biotinylated antibodies were performed in a 1xPBS solution containing 2% normal goat serum (NGS, Vector Laboratories, CA, USA) for those sections incubated with biotinylated anti-rabbit, and with 2% NGS and 2% normal rat serum for those incubated with biotinylated anti-mouse. Primary antibodies were incubated for 1 h at 37ºC and secondary antibodies at 37ºC for 30 min. Control slides were incubated without primary antibodies. After rinsing in 1xPBS at RT, the slides were incubated at 37ºC for 30 min in ABC solution (Vectastain Elite ABC Kit, Vector Laboratories) according to the manufacturer's procedures. The color reaction was performed with DAB solution I(0.05M Tris-HCl; 0.3mg/ml DAB (diaminobenzidine tetra hydrochloride, Sigma-Aldrich Chemie Gmbh); 10µl/ml DMSO (dimethyl sulfoxide, Sigma); 0.64mg/ml NaN_3 (Merck, Darmstadt, Germany)) and with DAB solution II (0.05M Tris-HCl; 0.3mg/ml DAB; 0.64mg/ml NaN_3; 0.06µl/ml H_2O_2 (Sigma-Aldrich Chemie Gmbh)) at RT for 5 min each. After rinsing in 1xPBS and in distilled water the sections were mounted in Mowiol (Calbiochem).

Preparation on figures

Photographs of the film autoradiograms of the hybridized tissue sections were taken with a Wild 420 Leica macroscope equipped with a digital camera (DXM1200 F, Nikon) and ACT-1 Nikon Software. Microphotography of the hybridized tissue slides was performed using a Zeiss Axioplan microscope equipped with a digital camera (DXM1200 F, Nikon) and ACT-1 Nikon Software. Figures were prepared for publication using Adobe Photoshop software (Adobe Software, San Jose, CA, USA). The contrast and brightness of images were the only variables adjusted digitally. For anatomical reference, sections close to those used were stained with cresyl violet.

RESULTS

Expression of cAMP-specific PDE enzymes in EAE rat brain

We first analyzed the expression pattern of the PDE4 and PDE7 isozymes at the lower brainstem level of 13-day EAE rats and compared them with control rats. The results are shown in the photographs in Fig.1. PDE4C expression was completely absent (Fig. 1E, F). PDE4A (Fig. 1A, B) and PDE4D (Fig. 1G, H) showed a similar hybridization pattern in both EAE and control rat brain. In contrast, PDE4B (Fig. 1C, D) expression presented additional dark patches of

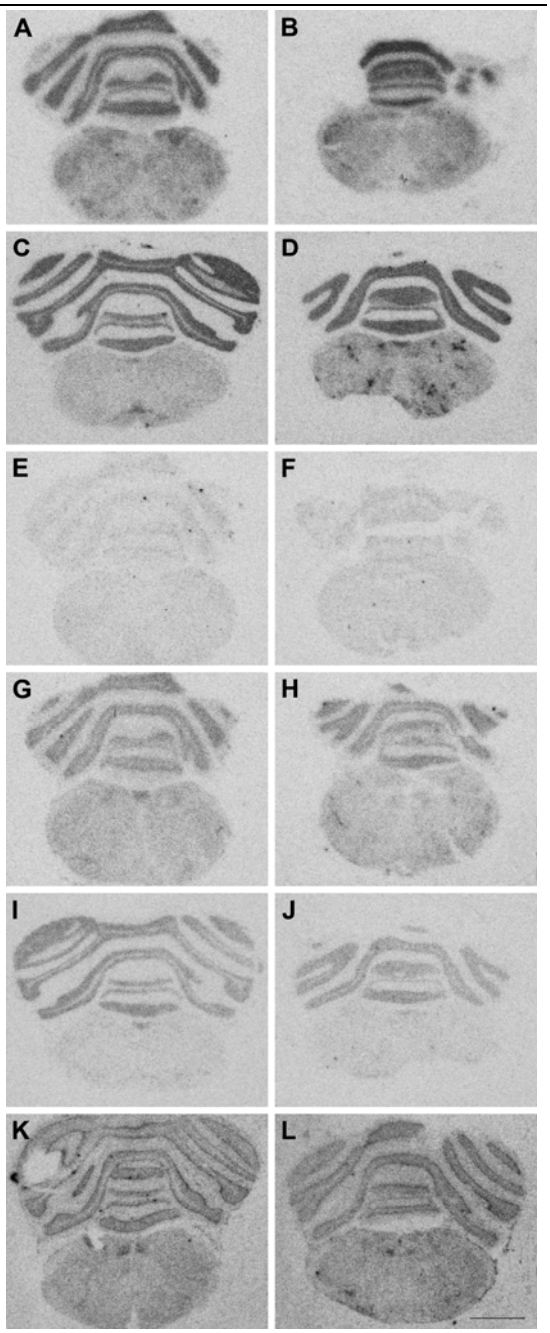

Figure 1. *cAMP-PDE mRNA expression in the brain of EAE rats.* Film autoradiogram images from rat coronal brain sections from control (A, C, E, G, I, K) and 13-day post-inoculation (B, D, F, H, J, L) obtained after *in situ* hybridization for mRNAs coding for PDE4A (A, B), PDE4B (C, D), PDE4C (E, F), PDE4D (G, H), PDE7A (I, J) and PDE7B (K, L). Note the dotted autoradiographic specific hybridization signal obtained for PDE4B mRNA after EAE induction (B_2). Bar = 2.5mm.

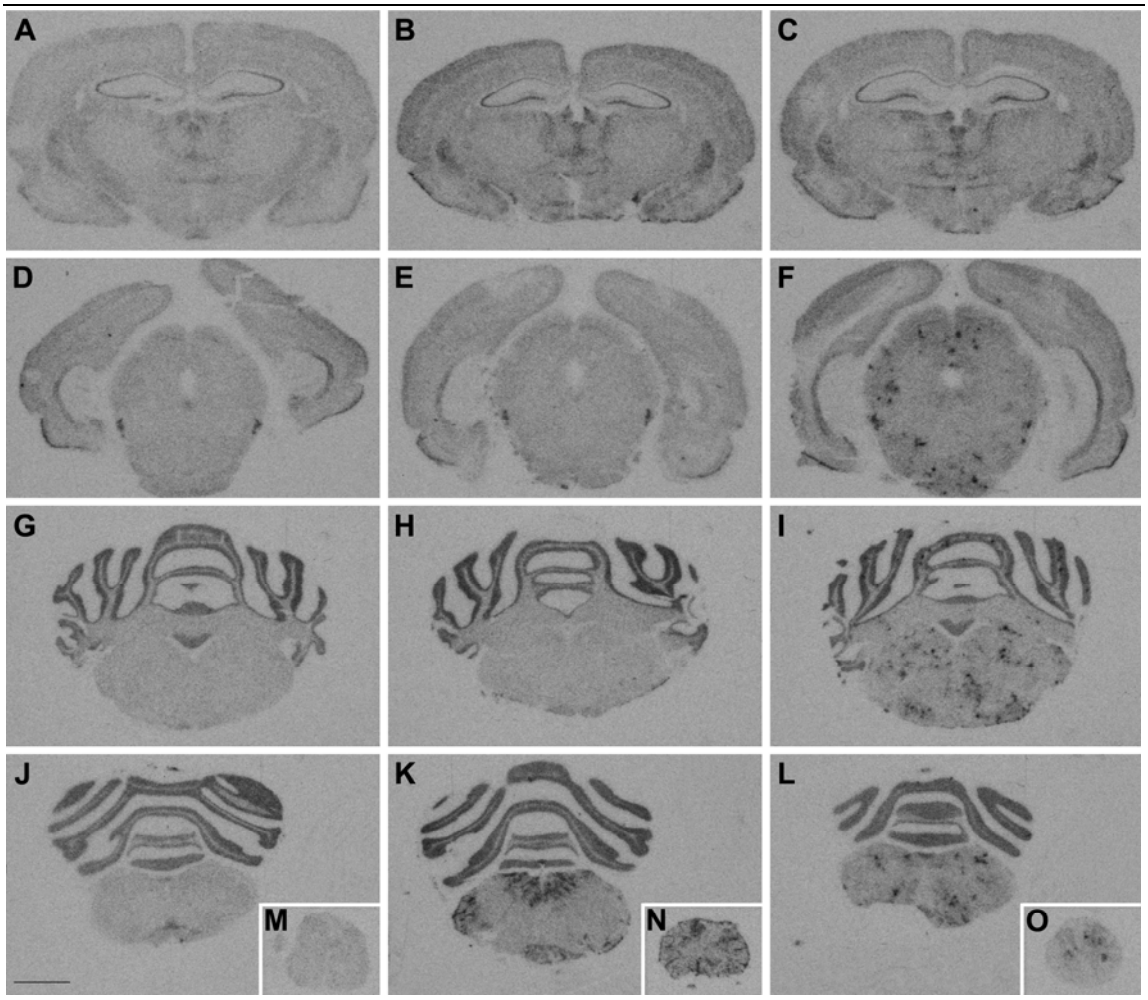

Figure 2. *PDE4B mRNA expression in EAE rat brain.* Film autoradiogram images from rat brain sections at four different coronal levels from control (A, D, G, J, M), 10-day (B, E, H, K, N) and 13-day (C, F, I, L, O) post-inoculation obtained after *in situ* hybridization to detect PDE4B mRNA. The accumulation of PDE4B can be observed from the spinal cord (O) to the midbrain level (F) in 13-day inoculated rats. Bar = 2.5 mm.

autoradiographic grains in a dispersed distribution only in EAE rats. No differences were observed in the expression of PDE7A (Fig. 1I, J) and PDE7B(Fig. 1K, L) between control and EAE brain.

Expression of PDE4B in EAE rat brain at different disease stages

Next, we analyzed the expression of PDE4B at different brain levels and at two different times of EAE induction, 10 days and 13 days post-inoculum. The results are shown in Fig. 2. The overexpression of PDE4B in EAE rats sacrificed 10 days after the inoculum (Fig. 2B, E, H, K, N) was limited to the lower parts of the brainstem. Hybridization levels were high from the spinal cord to the lower brainstem and the majority can be appreciated in the areas close to the brain ventricles. At a higher, anterior level, no abnormal PDE4B expression was seen. In contrast, when rats were sacrificed 13 days post-inoculum (Fig. 2C, F, I, L, O), the patchy distribution of PDE4B hybridization was seen from the spinal cord to more rostral brainstem levels. In this case this PDE4B overexpression was not concentrated close to the ventricles but rather extended throughout the microvasculature of the brainstem.

Expression of PDE4B splicing mRNA isoforms in EAE rat brain

Since PDE4B was the only PDE enzyme that showed an overexpression in EAE rat brain, our next step was to determine which of the four known PDE4B mRNA isoforms was responsible. The results are shown in Fig. 3, where PDE4B2 (Fig. 3B) was the only splicing variant that showed a similar hybridization pattern observed with the oligonucleotide probe that recognized all isoforms for PDE4B, as shown in Fig. 2L.

Identification of the cells containing the upregulated PDE4B2 mRNA

In order to identify the type of cells that overexpressed PDE4B2 mRNA in EAE rat

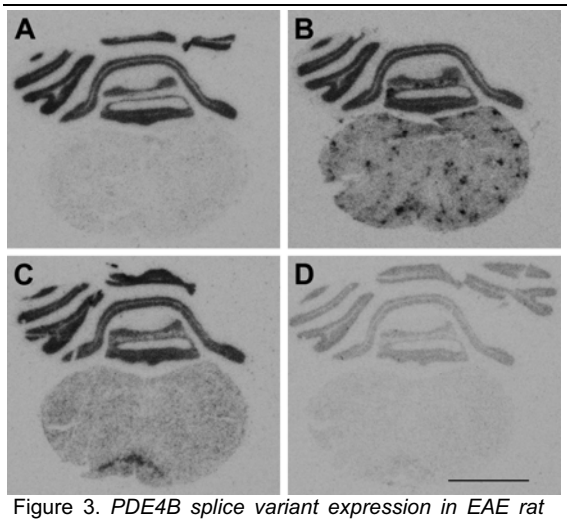

Figure 3. *PDE4B splice variant expression in EAE rat brain.* Film autoradiogram images from 13-day post-inoculum rat brain sections visualizing the mRNAs coding for PDE4B1 (A), PDE4B2 (B), PDE4B3 (C) and PDE4B4 (D). Bar = 3 mm.

brain, we performed the following experiments. First, we stained a coronal rat brain section with hematoxylin-eosine close to the section hybridized with the PDE4B2 oligonucleotide probe and found that most of the positive hybridizing cells were located in and close to brain vessels (not shown). We then performed double *in situ* hybridization experiments using a digoxigenin-labeled oligonucleotide complementary to the corresponding cell marker mRNA together with the radioactively labeled PDE4B2 probe. It was seen that the type of cells responsible for the up-regulation of PDE4B expression could not be assigned to a single population. Some brain T cells surrounding the brain vessels and some immediately adjacent to them, identified either by their hybridization with an oligonucleotide complementary to the T cell receptor active beta-chain C-region (TCRβ) mRNA (Fig. 4C) or by immunohistochemical reaction with an anti-CD3 antibody (Fig. 4D), expressed PDE4B2 mRNA. PDE4B2 mRNA was also found to be expressed in macrophages or microglia, identified by their hybridization with an oligonucleotide for the cell marker platelet–activating factor receptor (PAFR) (Fig. 4E) or by their reaction with an anti-CD11b antibody (Fig. 4F). Some T cells and some macrophages/microglia could be seen 10 days post-inoculum, close to the ventricular areas of the brainstem, whereas after 13 days cells were found in the parenchyma.

DISCUSSION

Using an animal model of multiple sclerosis, the EAE rat, we present the first description of the up-regulation of a PDE4B mRNA splice variant (PDE4B2) expression in the brain thus suggesting a possible involvement of this isoform in the development of the disease.

PDE7A has been found in both B cells (33) and T cells (in particular the alternative isoforms PDE7A1 and PDE7A3 (34)). A critical role of PDE7A in T cell proliferation and IL-2 production has been suggested by the use of specific antisense oligonucleotides which blocked these functions (35). This suggestion was reinforced by Nakata and coworkers, who found that T cell proliferation and cytokine synthesis was down-regulated by selective inhibition of PDE7A rather than PDE4 (36). However, the observation that PDE7A knockout mice (PDE7A $^{-/-}$) had functional T cells challenged previous hypotheses concerning the crucial role of this enzyme in T cell regulation (37). According to all these reports we expected to find PDE7A mRNA expression in the infiltrating T cells. Our observation on the lack of PDE7A expression in these T cells contradicts this prediction on the possible role that this phosphodiesterase could play in a T cell-mediated disease such as EAE. The reason for this discrepancy remains unexplained and deserves further work.

PDE4 isoenzymes have been considered a possible target for anti-inflammatory drugs due to their widespread expression pattern (in the central nervous system as well as in the periphery) and their involvement in the control of cell responses in inflammatory disease models, including EAE (21;38). In humans, circulating monocyte PDE4B gene expression is selectively induced by LPS (39;40). These results point to the possible role of PDE4B in inflammatory processes. Jin and coworkers (18-20) have shown, using either PDE4B or PDE4D knockout mice, that LPS stimulation of mouse inflammatory cells (peripheral leukocytes, peritoneal and lung macrophages) induced PDE4B mRNA accumulation and increased PDE4 activity. LPS-induced TNF-α secretion was lower in mice deficient in PDE4B but not in those lacking PDE4D, which indicates that the induction of PDE4B expression is essential for LPS-activated TNF-α responses. The authors suggest that, since there is no change in the cAMP levels in the cells deficient in PDE4B, a minor pool of cAMP regulated by PDE4B is involved in Toll-like receptor signaling.

Our results show a selective increase in

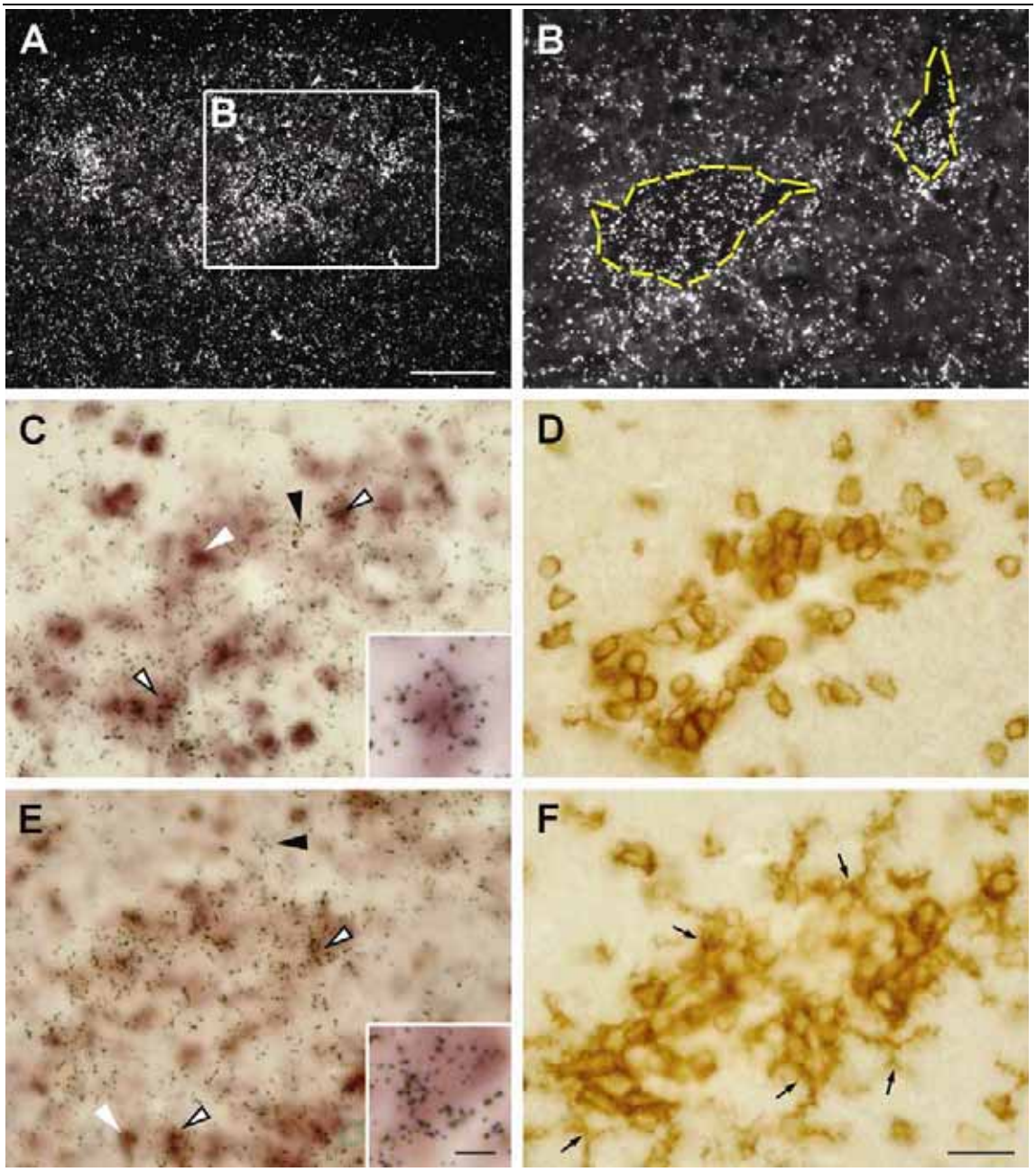

Figure 4. *PDE4B2 mRNA expression in T cells and macrophages/microglia around blood vessels of EAE rat cerebellar white matter.* A is a digital dark-field microphotograph of emulsion-dipped section, where hybridization signal for PDE4B2 mRNA is seen as white silver grains. B shows a higher magnification of A. Panels C and E are bright-field photomicrographs showing the simultaneous detection of PDE4B2 mRNA (dark silver grains) with a DIG-labeled oligonucleotide probe for TCRβ mRNA in some T cells (C) or with a DIG-labeled oligonucleotide probe for PAFR mRNA in some macrophages/microglia (E). White arrowheads point to cells positive for either DIG-TCRβ mRNA (C) or DIG-PAFR mRNA (E), black arrowheads mark cellular profiles positive for radioactively labeled PDE4B2 mRNA and black and white arrowheads show double labeled cells. Higher magnification displays double labeled cells (inset). Immunohistochemistry for CD3 to detect T cells (D) and CD-11b to detect macrophages/microglia (F) was performed on adjacent sections. Arrows in F point to some of the activated macrophages/microglia. Yellow lines in B mark the blood vessel limits. Bars A = 100 µm, B-F = 20 µm, and inset =5 µm.

PDE4B2 mRNA levels in the brain as a consequence of the induction of EAE in rats. We also observed a selective increase in PDE4B2 mRNA expression in some peripheral organs of LPS-treated rats (Reyes Irisarri and Mengod, unpublished data). This PDE4B2 behavior is consistent with that reported by other authors and discussed above for PDE4 in the periphery of some animal inflammation models and bears out the conclusion of Jin and coworkers (18) that PDE4B2 is the major PDE4 form inducible by LPS (in their case), and the only form induced by autoimmune neuroinflammation of EAE rats (present results). The activation of resident microglia and perivascular macrophages and the recruitment of T cells in the central nervous system (41;42) are among the most consistent

changes observed in EAE rats. We observed that the increase in PDE4B occurs in T cells and macrophages or microglia, which suggests that this isoenzyme is directly involved in EAE disease and that its function in these cells is highly specialized.

The PDE4B2 mRNA induction observed mainly in infiltrated T cells and macrophages/microglia in EAE rat brain seems to coincide with the peak of the expression observed for several cytokines, TNF-α, IFN-γ, LT, IL-β and TGF-β (22;43;44) on day 13 in the same animal model. This upregulation of PDE4B2 expression observed is also probably located in activated macrophages or microglia cells, due to the morphology of the cells and to the fact that "resting" microglia in control brain do not express this isoform. Taken together, these findings suggest that the induction of PDE4B2 expression in the cellular infiltrates of EAE rat brain could be necessary for cytokine production.

Stimulation of T cells through their antigen receptors (TCRs) produces a marked increase in intracellular cAMP levels, most probably due to the activation of adenylate cyclase by a G protein coupled to the TCR (45). However, high levels of cAMP inhibit many of the biological responses of the T cell (35), so antigen receptor-mediated signaling must be coordinated with the activation of PDEs. There is evidence of the involvement of a biochemical pathway in the coordination of cAMP-PDE activation to limit the magnitude and the duration of the increase in cAMP levels resulting from the TCR signaling (46). Arp and coworkers have recently shown that *de novo* expression of PDE4B2, previously shown to be associated with the CD3ε chain of TCR (47), enhances T cell activation and increases IL-2 production (48). This effect correlates with the intracellular distribution of PDE4B2, found within lipid rafts following T cell stimulation. The authors propose that a compartmentalization of PDE4B2 occurs close to the immunological synapse and sites of maximal cAMP generation at early T cell activation times. Another compartmentalization has been proposed for PDE4s, but particularly for PDE4D5, which interact with β-arrestin, thereby recruiting PDEs to ligand-activated receptors (49). Such an interaction provides a mechanism by which cAMP-degrading enzymes can be delivered close to the point of cAMP production in an agonist-dependent fashion. In this way, compartmentalized PDEs may be recruited to different areas of the cell where they can be involved in different signaling pathways (50). Consequently, the induction of PDE4B2 observed in our study suggest that this isoform could be located in precise compartments in the infiltrating cells, helping to maintain low cAMP levels in the microcompartments and thus allowing full activation of the cytokine responses. Preliminary data obtained in our laboratory from EAE rats treated with rolipram according to the protocol established by Sanchez and coworkers (51) show a decrease in the number of cellular infiltrates, which correlates well with the absence of the PDE4B2 overexpression (data not shown) described above and that is characteristic of this model.

In summary, in the present work we described an up-regulation in the expression of one of the PDE4B splicing variants (PDE4B2) in the T cells and in macrophages/microglia in perivascular cuffs and parenchyma in the spinal cord and brainstem of rats with EAE. These findings have important physiological consequences and are indicative of a very precise and specialized role of PDE4B2 in some cellular subpopulations. These results support the role played by PDE4B2 in inflammation and its importance as a therapeutic target for the treatment of neuroinflammatory diseases using subtype-selective PDE4B inhibitors.

AKNOWLEDGMENTS

We wish to thank Rocío Martín for technical assistance and Robin Rycroft for English corrections.

REFERENCE LIST

1. Lassmann H. Mechanisms of demyelination and tissue destruction in multiple sclerosis. Clin Neurol Neurosurg 2002;104:168-71
2. Lassmann H, Bruck W, Lucchinetti C. Heterogeneity of multiple sclerosis pathogenesis: implications for diagnosis and therapy. Trends Mol Med 2001;7:115-21
3. Link H, Xiao BG. Rat models as tool to develop new immunotherapies. Immunol Rev 2001;184:117-28
4. Brok HP, Bauer J, Jonker M, et al. Non-human primate models of multiple sclerosis. Immunol Rev 2001;183:173-85
5. Sospedra M, Martin R. Immunology of multiple sclerosis. Annu Rev Immunol 2005;23:683-747

6. Gay FW, Drye TJ, Dick GW, et al. The application of multifactorial cluster analysis in the staging of plaques in early multiple sclerosis. Identification and characterization of the primary demyelinating lesion. Brain 1997;120:1461-83
7. Trapp BD, Peterson J, Ransohoff RM, et al. Axonal transection in the lesions of multiple sclerosis. N Engl J Med 1998;338:278-85
8. Van Wauwe J, Aerts F, Walter H, et al. Cytokine production by phytohemagglutinin-stimulated human blood cells: effects of corticosteroids, T cell immunosuppressants and phosphodiesterase IV inhibitors. Inflamm Res 1995;44:400-5
9. Giembycz MA, Dent G. Prospects for selective cyclic nucleotide phosphodiesterase inhibitors in the treatment of bronchial asthma. Clin Exp Allergy 1992;22:337-44
10. Bender AT, Beavo JA. Cyclic nucleotide phosphodiesterases: molecular regulation to clinical use. Pharmacol Rev 2006;58:488-520
11. Miró X, Pérez-Torres S, Puigdomènech P, et al. Differential distribution of PDE4D splice variant mRNAs in rat brain suggests association with specific pathways and presynaptical localization. Synapse 2002;45:259-69
12. Pérez-Torres S, Miró X, Palacios JM, et al. Phosphodiesterase type 4 isozymes expression in human brain examined by *in situ* hybridization histochemistry and[^{3}H]rolipram binding autoradiography. Comparison with monkey and rat brain. J Chem Neuroanat 2000;20:349-74
13. Miró X, Pérez-Torres S, Palacios JM, et al. Differential distribution of cAMP-specific phosphodiesterase 7A mRNA in rat brain and peripheral organs. Synapse 2001;40:201-14
14. Pérez-Torres S, Cortés R, Tolnay M, et al. Alterations on phosphodiesterase type 7 and 8 isozyme mRNA expression in Alzheimer's disease brains examined by in situ hybridization. Exp Neurol 2003;182:322-34
15. Reyes-Irisarri E, Perez-Torres S, Mengod G. Neuronal expression of cAMP-specific phosphodiesterase 7B mRNA in the rat brain. Neuroscience 2005;132:1173-85
16. Houslay MD, Sullivan M, Bolger GB. The multienzyme PDE4 cyclic adenosine monophosphate-specific phosphodiesterase family: intracellular targeting, regulation, and selective inhibition by compounds exerting anti-inflammatory and antidepressant actions. Adv Pharmacol 1998;44:225-342
17. Schudt C, Tenor H, Hatzelmann A. PDE isoenzymes as targets for anti-asthma drugs. Eur Respir J 1995;8:1179-83
18. Jin SL, Conti M. Induction of the cyclic nucleotide phosphodiesterase PDE4B is essential for LPS-activated TNF-alpha responses. Proc Natl Acad Sci U S A 2002;99:7628-33
19. Ariga M, Neitzert B, Nakae S, et al. Nonredundant function of phosphodiesterases 4D and 4B in neutrophil recruitment to the site of inflammation. J Immunol 2004;173:7531-8
20. Jin SL, Lan L, Zoudilova M, et al. Specific role of phosphodiesterase 4B in lipopolysaccharide-induced signaling in mouse macrophages. J Immunol 2005;175:1523-31
21. Sommer N, Loschmann PA, Northoff GH, et al. The antidepressant rolipram suppresses cytokine production and prevents autoimmune encephalomyelitis. Nat Med 1995;1:244-8
22. Martinez I, Puerta C, Redondo C, et al. Type IV phosphodiesterase inhibition in experimental allergic encephalomyelitis of Lewis rats: sequential gene expression analysis of cytokines, adhesion molecules and the inducible nitric oxide synthase. J Neurol Sci 1999;164:13-23
23. Moore CS, Earl N, Frenette R, et al. Peripheral phosphodiesterase 4 inhibition produced by 4-[2-(3,4-Bis-difluoromethoxyphenyl)-2-[4-(1,1,1,3,3,3-hexafluoro-2-hydrox ypropan-2-yl)-phenyl]-ethyl]-3-methylpyridine-1-oxide (L-826,141) prevents experimental autoimmune encephalomyelitis. J Pharmacol Exp Ther 2006;319:63-72
24. Dinter H, Onuffer J, Faulds D, et al. Phosphodiesterase type IV inhibitors in the treatment of multiple sclerosis. J Mol Med 1997;75:95-102
25. Dyke HJ, Montana JG. Update on the therapeutic potential of PDE4 inhibitors. Exp Opin Invest Drugs 2002;11:1-13
26. Dinter H, Tse J, Halks-Miller M, et al. The type IV phosphodiesterase specific inhibitor mesopram inhibits experimental autoimmune encephalomyelitis in rodents. J Neuroimmunol 2000;108:136-46
27. Puerta C, Martinez I, Baranda P, et al. Aminoguanidine reduces apoptosis of circulating V Beta 8.2 T lymphocytes in Lewis rats with actively induced experimental autoimmune encephalomyelitis. Association with persistent inflammation of the central nervous system and lack of recovery. J Neuroimmunol 2000;110:140-50
28. Pompeiano M, Palacios JM, Mengod G. Distribution and cellular localization of mRNA coding for 5-HT1A receptor in the rat brain: correlation with receptor binding. J Neurosci 1992;12:440-53
29. Schmitz GG, Walter T, Seibl R, et al. Nonradioactive labeling of oligonucleotides in vitro with the hapten digoxigenin by tailing with terminal transferase. Anal Biochem 1991;192:222-31
30. Tomiyama M, Palacios JM, Cortés R, et al. Distribution of AMPA receptor subunit mRNAs in the human basal ganglia: an in situ hybridization study. Mol Brain Res 1997;46:281-9
31. Landry M, Holmberg K, Zhang X, et al. Effect of axotomy on expression of NPY, galanin, and NPY Y1 and Y2 receptors in dorsal root ganglia and the superior cervical ganglion studied with double-labeling in situ hybridization and immunohistochemistry. Exp Neurol 2000;162:361-84

32. Serrats J, Artigas F, Mengod G, et al. GABAB receptor mRNA in the raphe nuclei: co-expression with serotonin transporter and glutamic acid decarboxylase. J Neurochem 2003;84:743-52
33. Lee R, Wolda S, Moon E, et al. PDE7A is expressed in human B-lymphocytes and is up-regulated by elevation of intracellular cAMP. Cell Signal 2002;14:277-84
34. Smith SJ, Brookes-Fazakerley S, Donnelly LE, et al. Ubiquitous expression of phosphodiesterase 7A in human proinflammatory and immune cells. Am J Physiol Lung Cell Mol Physiol 2003;284:L279-L289
35. Li L, Yee C, Beavo JA. CD3- and CD28-dependent induction of PDE7 required for T cell activation. Science 1999;283:848-51
36. Nakata A, Ogawa K, Sasaki T, et al. Potential role of phosphodiesterase 7 in human T cell function: comparative effects of two phosphodiesterase inhibitors. Clin Exp Immunol 2002;128:460-6
37. Yang G, McIntyre KW, Townsend RM, et al. Phosphodiesterase 7A-deficient mice have functional T cells. J Immunol 2003;171:6414-20
38. Genain CP, Roberts T, Davis RL, et al. Prevention of autoimmune demyelination in non-human primates by a cAMP- specific phosphodiesterase inhibitor. Proc Natl Acad Sci U S A 1995;92:3601-5
39. Ma D, Wu P, Egan RW, et al. Phosphodiesterase 4B gene transcription is activated by lipopolysaccharide and inhibited by interleukin-10 in human monocytes. Mol Pharmacol 1999;55:50-7
40. Verghese MW, McConnell RT, Lenhard JM, et al. Regulation of distinct cyclic AMP-specific phosphodiesterase (phosphodiesterase type 4) isozymes in human monocytic cells. Mol Pharmacol 1995;47:1164-71
41. Polman CH, Dijkstra CD, Sminia T, et al. Immunohistological analysis of macrophages in the central nervous system of Lewis rats with acute experimental allergic encephalomyelitis. J Neuroimmunol 1986;11:215-22
42. Sobel RA, Blanchette BW, Bhan AK, et al. The immunopathology of experimental allergic encephalomyelitis. I. Quantitative analysis of inflammatory cells in situ. J Immunol 1984;132:2393-401
43. Issazadeh S, Ljungdahl A, Hojeberg B, et al. Cytokine production in the central nervous system of Lewis rats with experimental autoimmune encephalomyelitis: dynamics of mRNA expression for interleukin-10, interleukin-12, cytolysin, tumor necrosis factor alpha and tumor necrosis factor beta. J Neuroimmunol 1995;61:205-12
44. Issazadeh S, Mustafa M, Ljungdahl A, et al. Interferon gamma, interleukin 4 and transforming growth factor beta in experimental autoimmune encephalomyelitis in Lewis rats: dynamics of cellular mRNA expression in the central nervous system and lymphoid cells. J Neurosci Res 1995;40:579-90
45. Kammer GM, Boehm CA, Rudolph SA, et al. Mobility of the human T lymphocyte surface molecules CD3, CD4, and CD8: regulation by a cAMP-dependent pathway. Proc Natl Acad Sci U S A 1988;85:792-6
46. Giembycz MA, Corrigan CJ, Seybold J, et al. Identification of cyclic AMP phosphodiesterases 3, 4 and 7 in human CD4+ and CD8+ T-lymphocytes: role in regulating proliferation and the biosynthesis of interleukin-2. Br J Pharmacol 1996;118:1945-58
47. Baroja ML, Cieslinski LB, Torphy TJ, et al. Specific CD3 epsilon association of a phosphodiesterase 4B isoform determines its selective tyrosine phosphorylation after CD3 ligation. J Immunol 1999;162:2016-23
48. Arp J, Kirchhof MG, Baroja ML, et al. Regulation of T-cell activation by phosphodiesterase 4B2 requires its dynamic redistribution during immunological synapse formation. Mol Cell Biol 2003;23:8042-57
49. Perry SJ, Baillie GS, Kohout TA, et al. Targeting of cyclic AMP degradation to beta 2-adrenergic receptors by beta-arrestins. Science 2002;298:834-6
50. Iyengar R. Gating by cyclic AMP: expanded role for an old signaling pathway. Science 1996;271:461-3
51. Sanchez AJ, Puerta C, Ballester S, et al. Rolipram impairs NF-kappaB activity and MMP-9 expression in experimental autoimmune encephalomyelitis. J Neuroimmunol 2005;168:13-20